# Measurements of Magnetic Field Penetration of Materials for Superconducting Radiofrequency (SRF) Cavities

**Harshani Senevirathne**[1,2] **,** A-M Valente-Feliciano[2], A. Gurevich[1], J. R. Delayen[1,2]

[1]Center for Accelerator Science, Old Dominion University, USA

[2]Thomas Jefferson National Accelerator Facility, USA

May 11, 2023

# Introduction

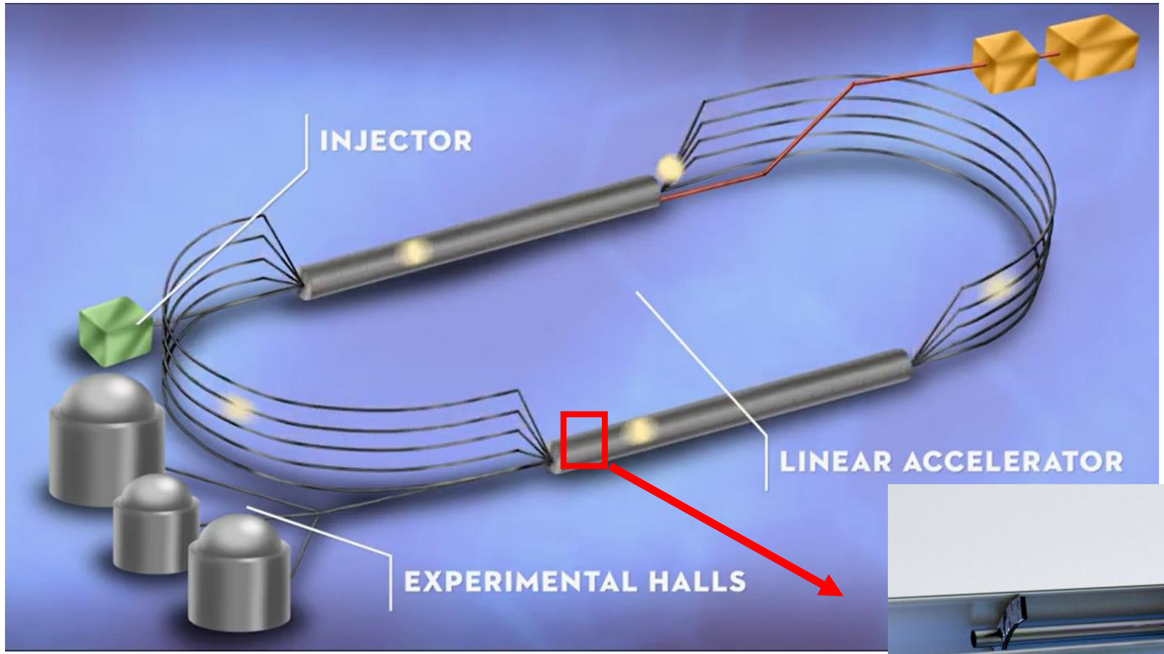


CEBAF, Jefferson Lab

Typical SRF cavities are made out of Nb

41
Nb
Niobium
92.90637

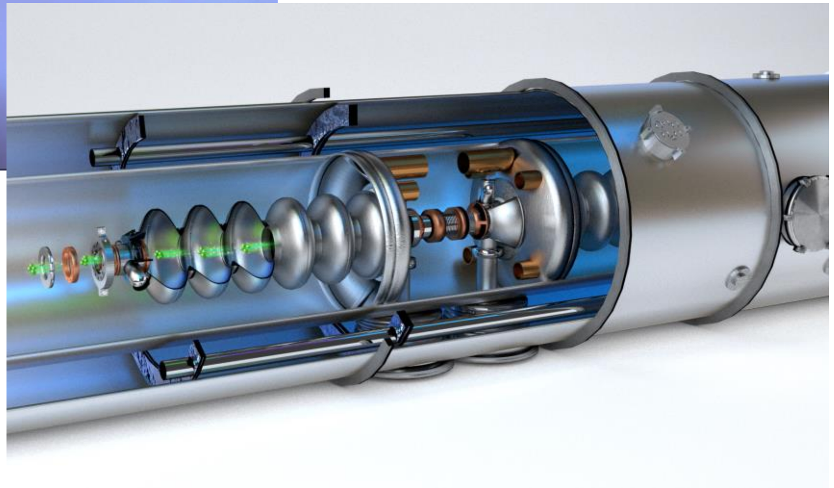

Superconducting RF accelerating cavity is a key component of the particle accelerators which impart energy to charged particles

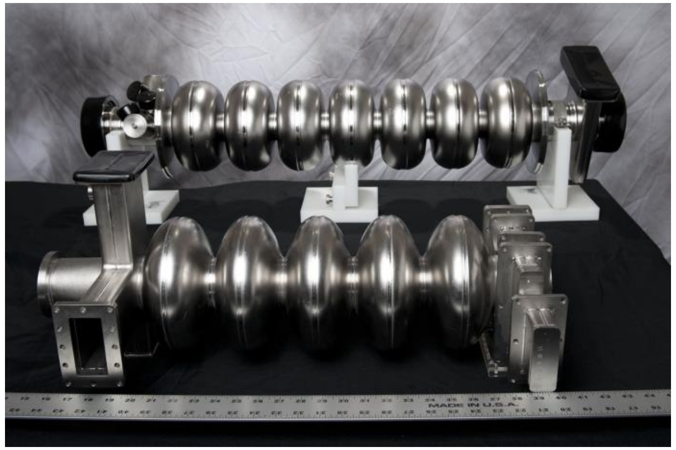

five- and seven-cell niobium cavities produced at Jefferson Lab's SRF Institute

The key figures of merit that are used to evaluate SRF cavities are,

- Quality factor ($Q_0$)
- Accelerating gradient, ($E_{acc}$)
  - Peak surface magnetic Field ($B_{pk}$)

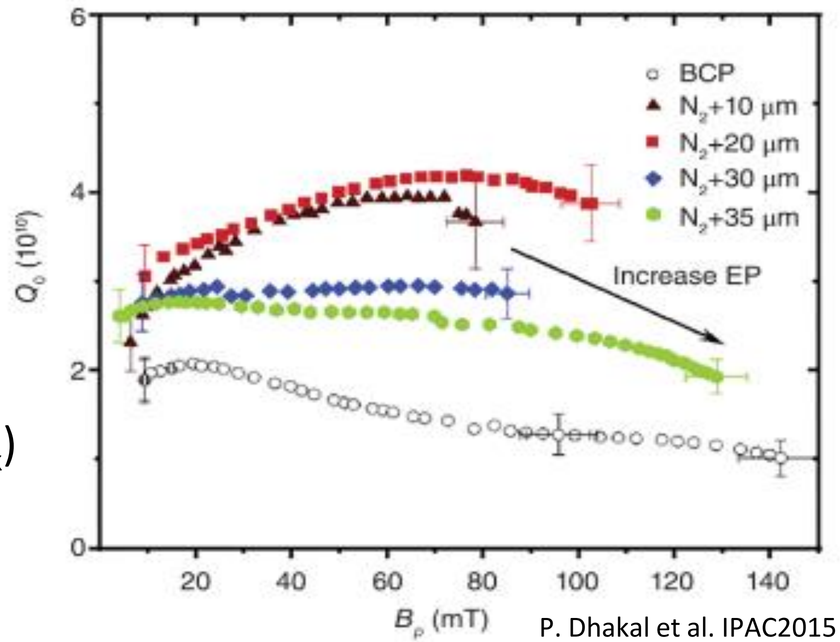


P. Dhakal et al. IPAC2015

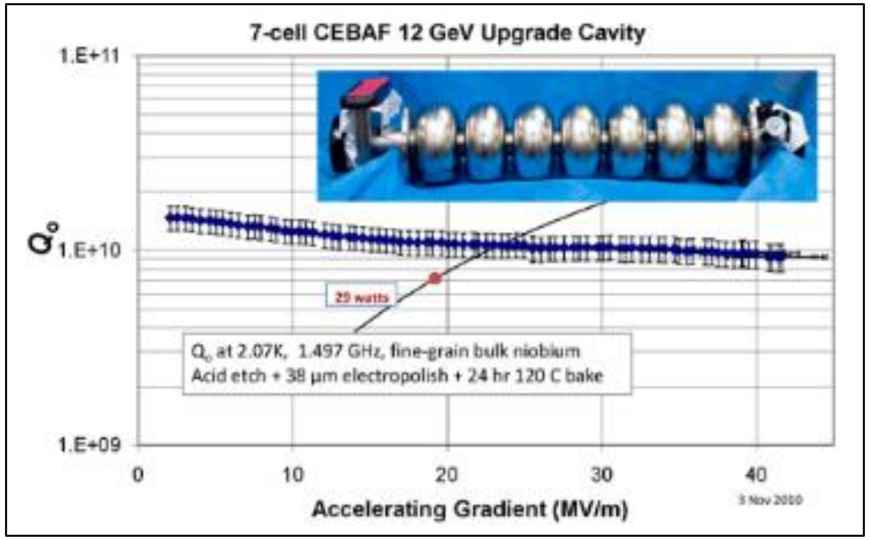


C. E. Reece and G. Ciovati Rev of Acce. Sci. and Tech. Vol. 05, pp. 285-312 (2012)

The ratio of the stored energy to power disipation , $Q_o = \frac{\omega_o U}{P_c} \propto 1/R_s$

The ratio of the accelerating voltage per cell $V$ to the cell length, $E_{acc}(MV/m) = \frac{V}{L} \propto B_{pk}$ (mT)

Peak Surface Magnetic Field

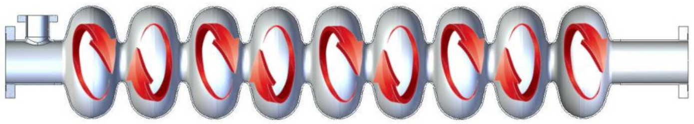

# Why new materials ?

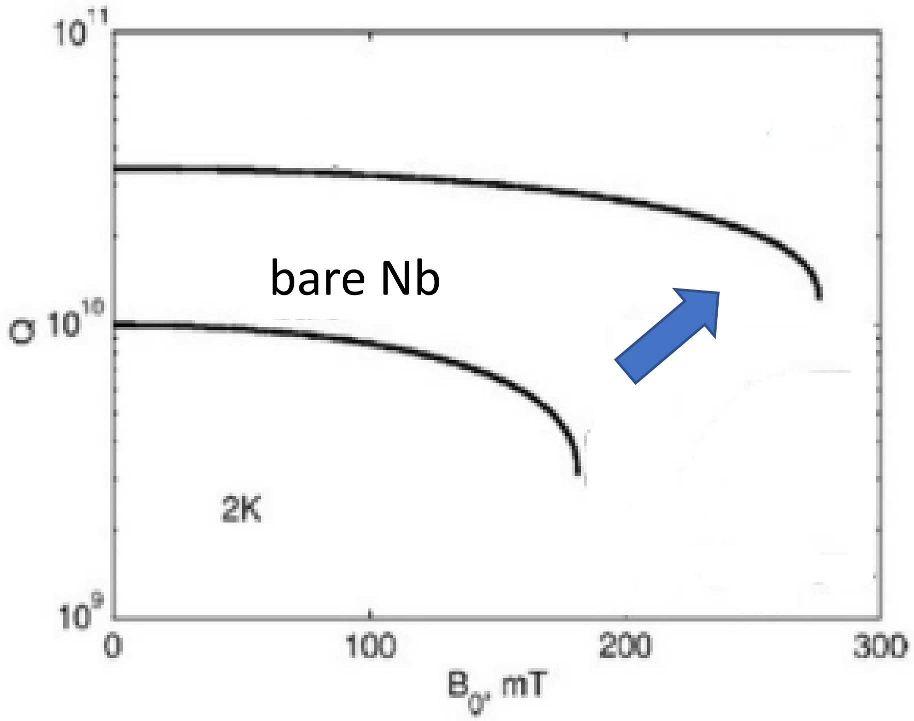


Nb SRF cavities can achieve

- High quality factor ~ $10^{10}$-$10^{11}$
- High Accelerating gradient ~52 $MVm^{-1}$ (at 1.3–2 K and 1–2 GHz)
- Peak surface magnetic field has reached close to its theoretical limit

  $H_{max} \approx H_c = 200$ mT

For further improved RF performance of the cavity, materials other than Nb are needed to characterize.

# What Choices for New Material ?

Choices are based on,

- Higher $T_c$ } Low Rs→ For low RF losses → High Quality Factor; Increase cavity operation temperature from 2 K to 4 K

$$Q_o \;\alpha\; \frac{1}{R_s}$$

- Higher $H_c$
- Higher $H_{c1}$

} For high accelerating gradients

$$E_{acc} \;\alpha\; B_{pk}$$

# Field Penetration into Type II Superconductor

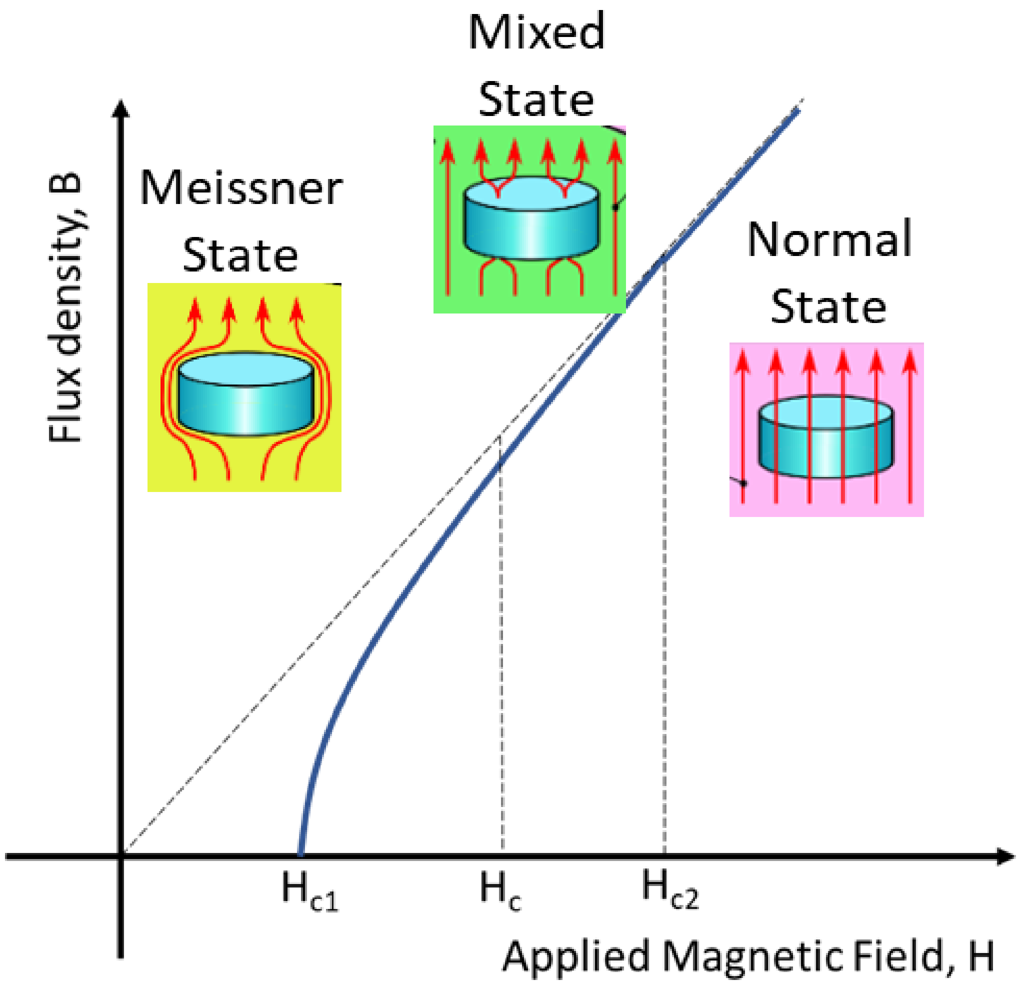


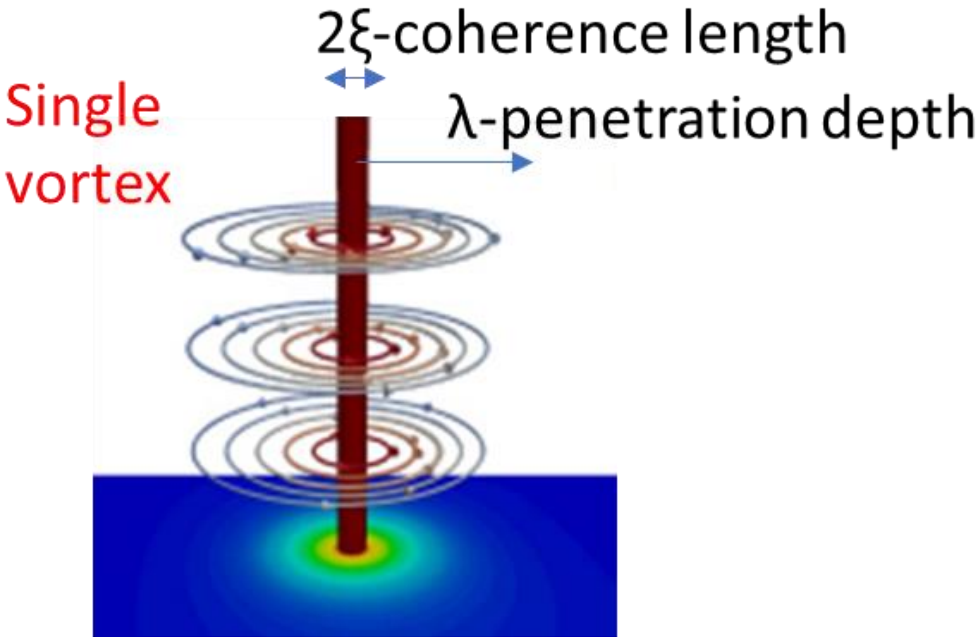

# In Type – II superconductors, the Meissner state can persist metastably above $H_{c1}$ but only up to $H_{sh}$

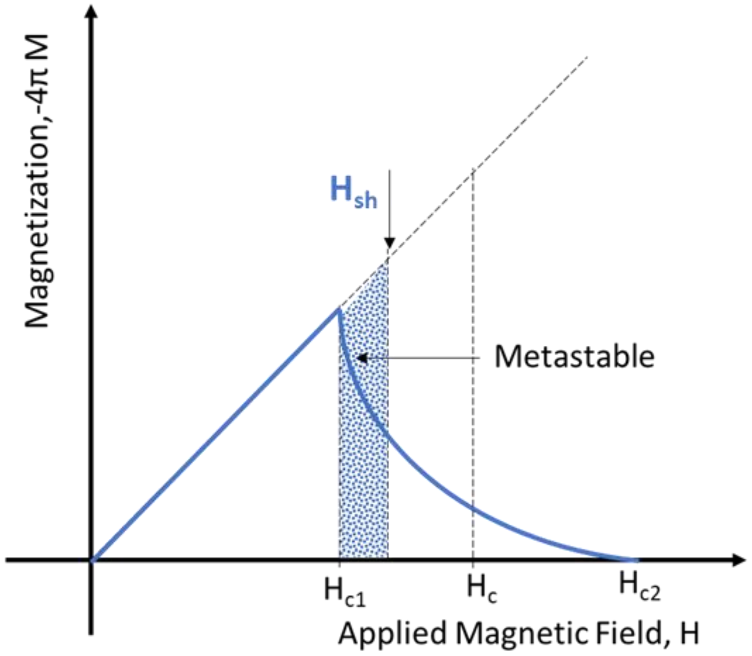


Gibbs free energy of isolated vortex

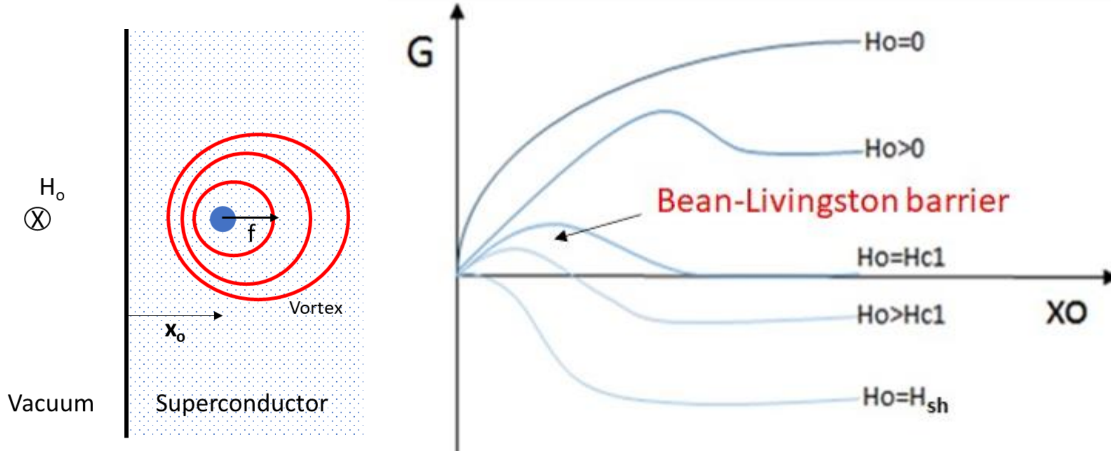


Single vortex near ideal surface parallel to external field

Optical Image of BCP Nb

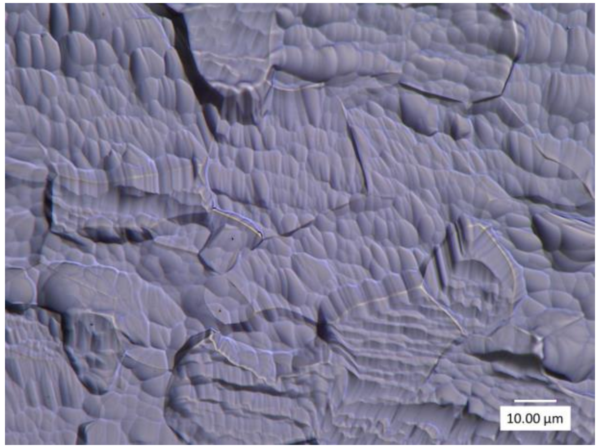


- Vortices have to overcome surface barrier even at $H > H_{c1}$
- Surface barrier vanishes at superheating field $H_{sh}$
- Surface barrier weaken at defects and vanishes at **$H = H_p$** where **$H_{c1} < H_p < H_{sh}$** even at **$H_p < H_{c1}$**
- **Early flux penetration limits the SRF cavity performances at higher fields**

# SIS Multilayers on Nb : Shield Nb at high surface magnetic field

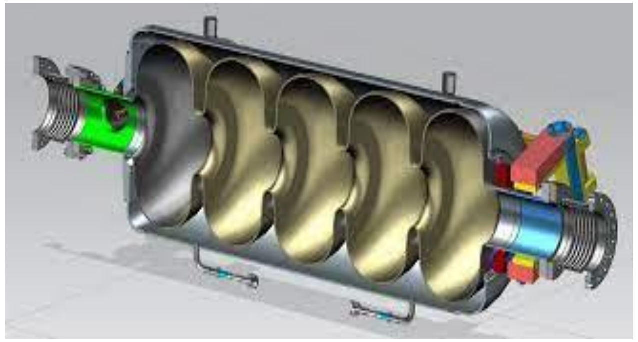

Half of the multicell cavity showing inner view

\+

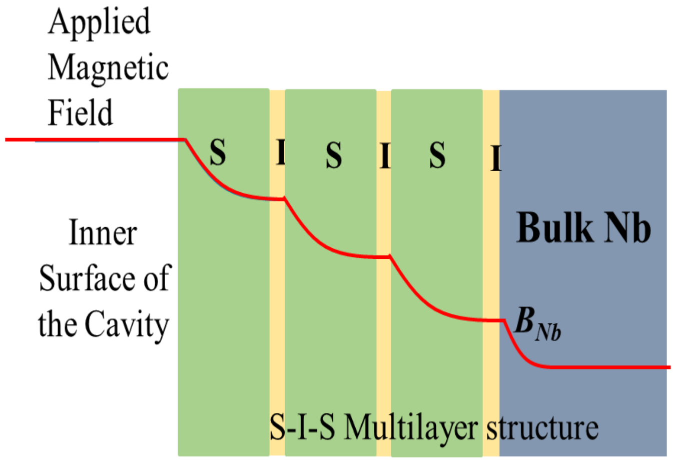


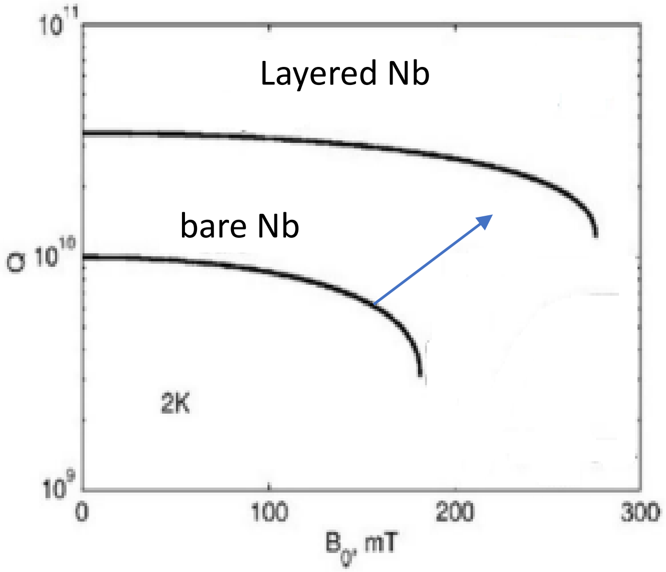


- $Nb_3Sn$
- NbN
- NbTiN
- Pnictides
- Alloyed Nb…

**S**

- $Al_2O_3$
- MgO
- AlN…

**I**

Thin SC layer (< λ) → $H_p$↑ →Vortex enter at higher field
→ allows high magnetic field inside the cavity
→ Shield Nb surface
→ higher $E_{acc}$

# Objective of the project

- **Surface field at onset of flux penetration, $B_p$** is a useful characteristic to explore the shielding effect of SIS multilayers.
- Techniques to measure the onset of magnetic field penetration into superconducting samples need to be developed emulating the field profile at wall of the SRF cavity operating at fundamental accelerating mode.
- In this project, Magnetic Field Penetration (MFP) Magnetometer was designed, built and then implemented for measurements at Jefferson Lab.

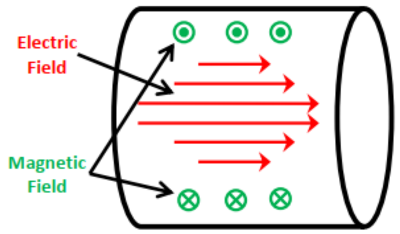


fundamental accelerating mode $TM_{010}$ used for acceleration

# Magnetic Field Penetration (MFP) Magnetometer

To investigate the shielding effect of multilayers, Magnetic Field Penetration (MFP) magnetometer is designed, built and implementing for magnetic field penetration measurements.

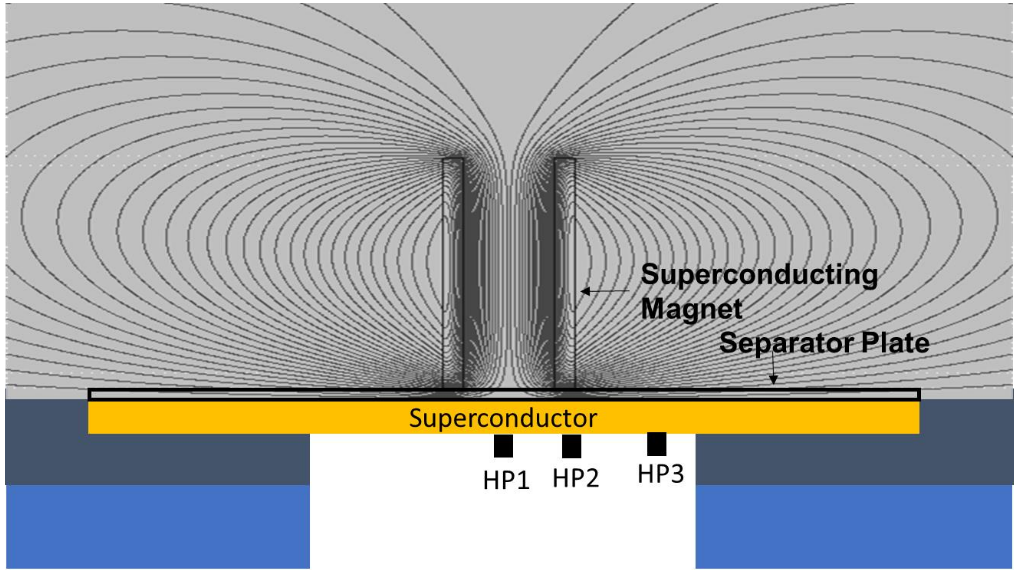


Basic Experimental Setup

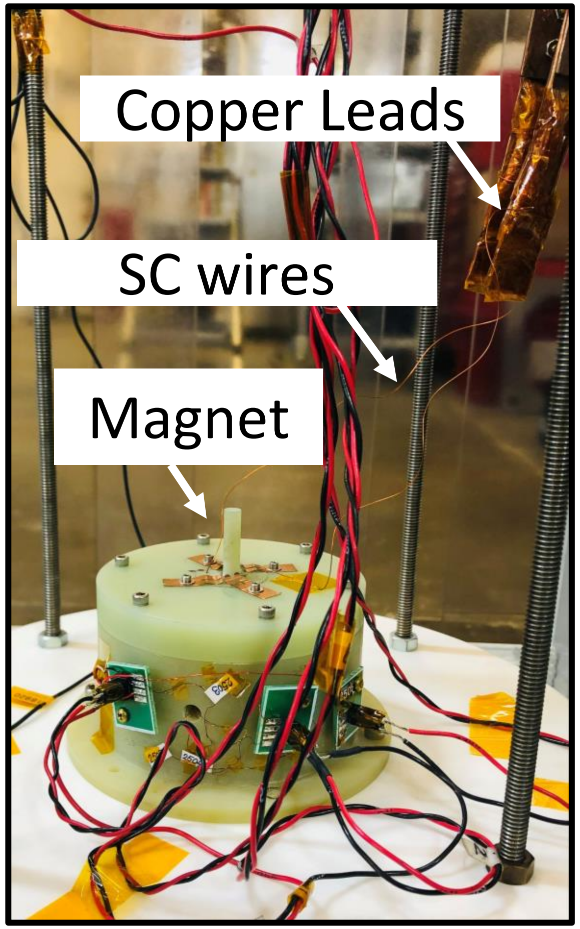


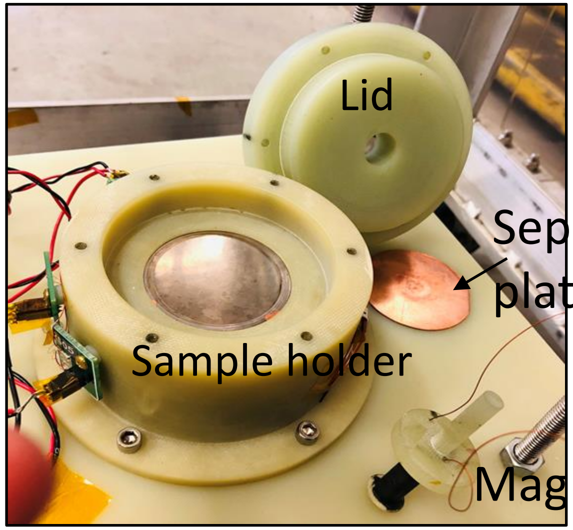


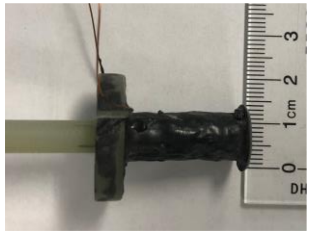

Magnet

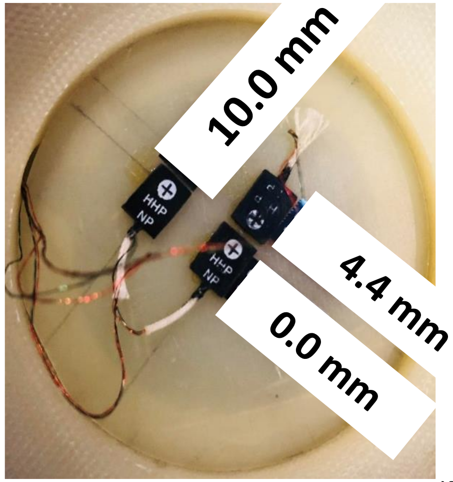


Hall probes

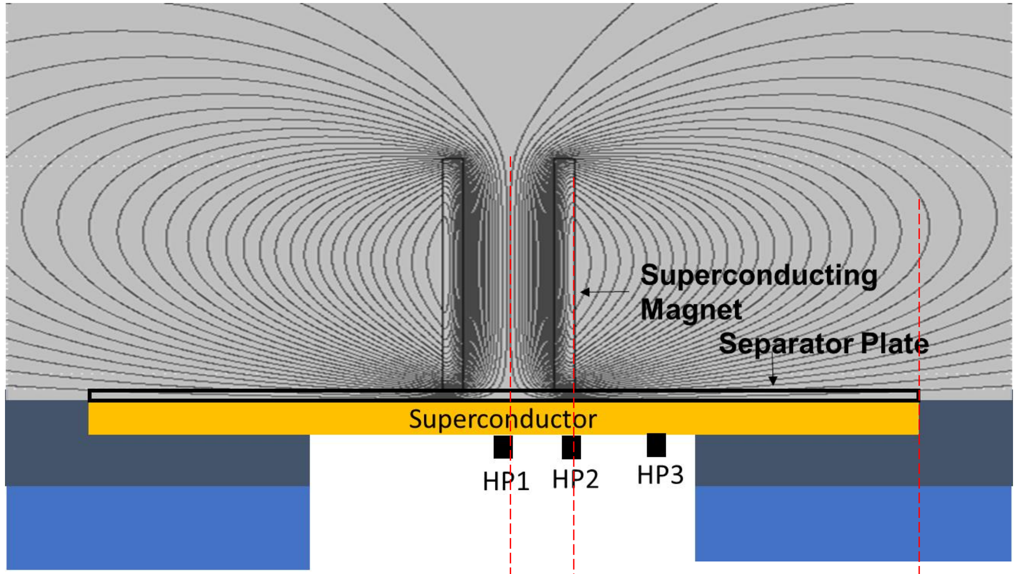


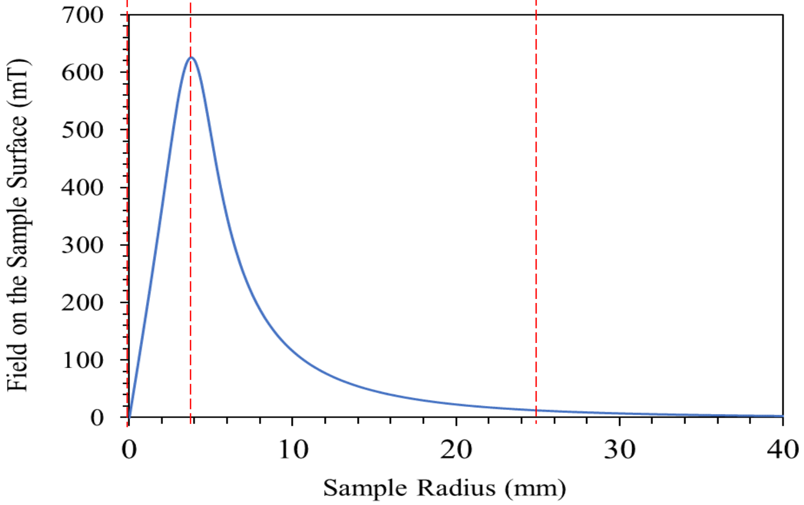


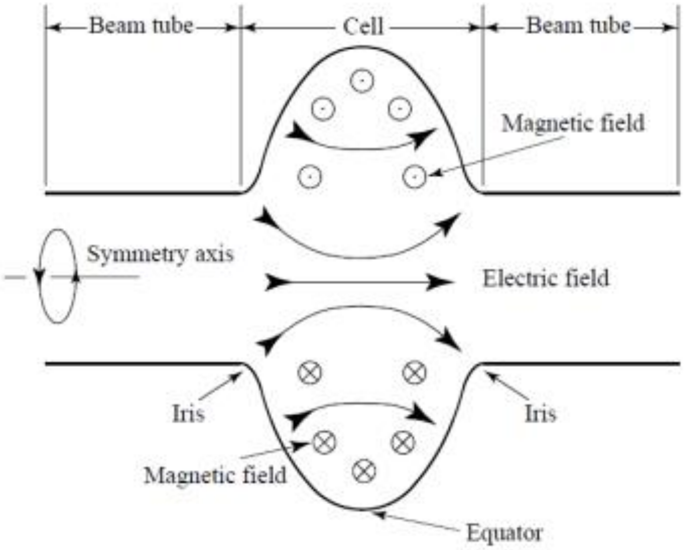


Peak Magnetic field

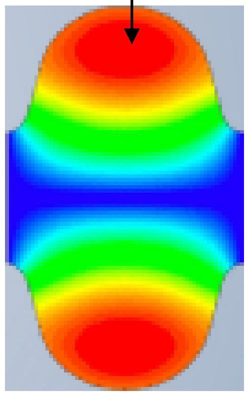

- In the Meissner state, sample act as a magnetic mirror.
- A current is generated at the surface of the superconductor in order to cancel the applied field at the surface.
- The combined applied and induced fields result is parallel to the sample surface, which resembles the magnetic field profile at the equator of the accelerating cavity.

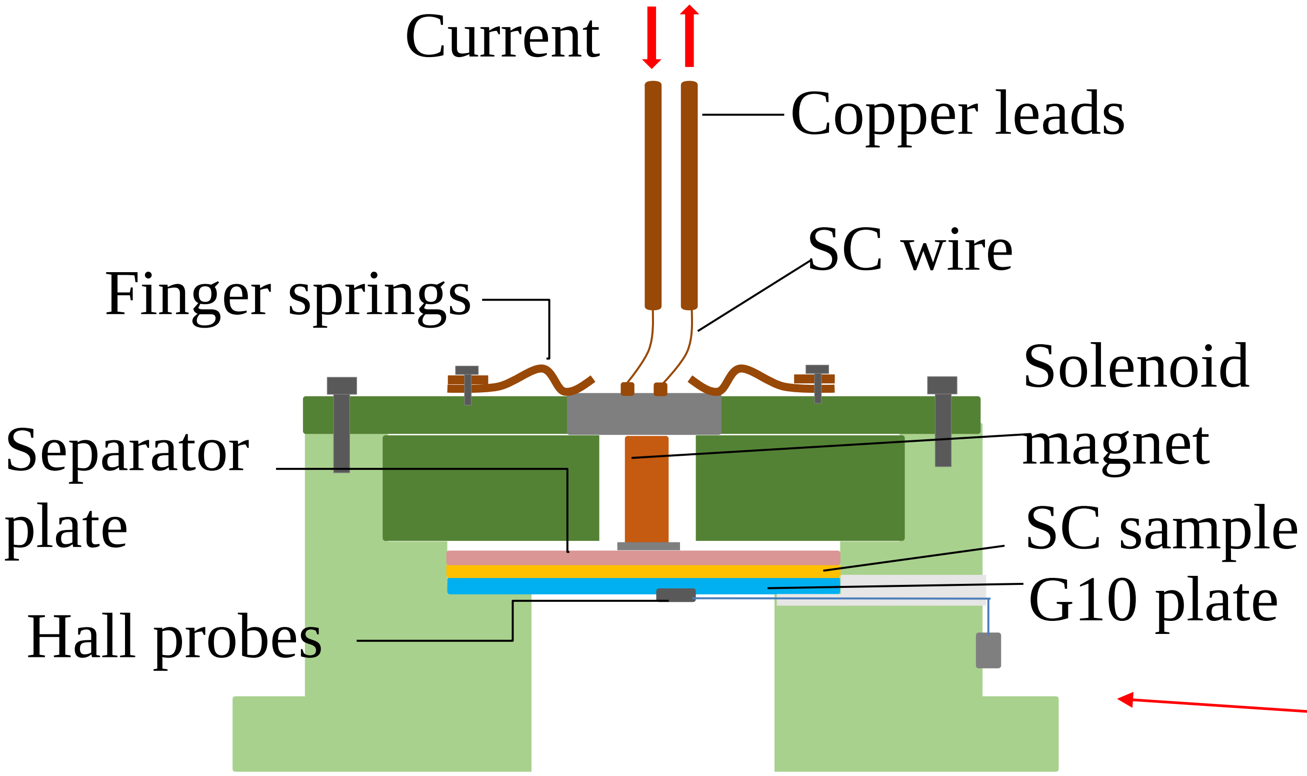
Current
Copper leads
SC wire
Finger springs
Solenoid magnet
Separator plate
SC sample
G10 plate
Hall probes

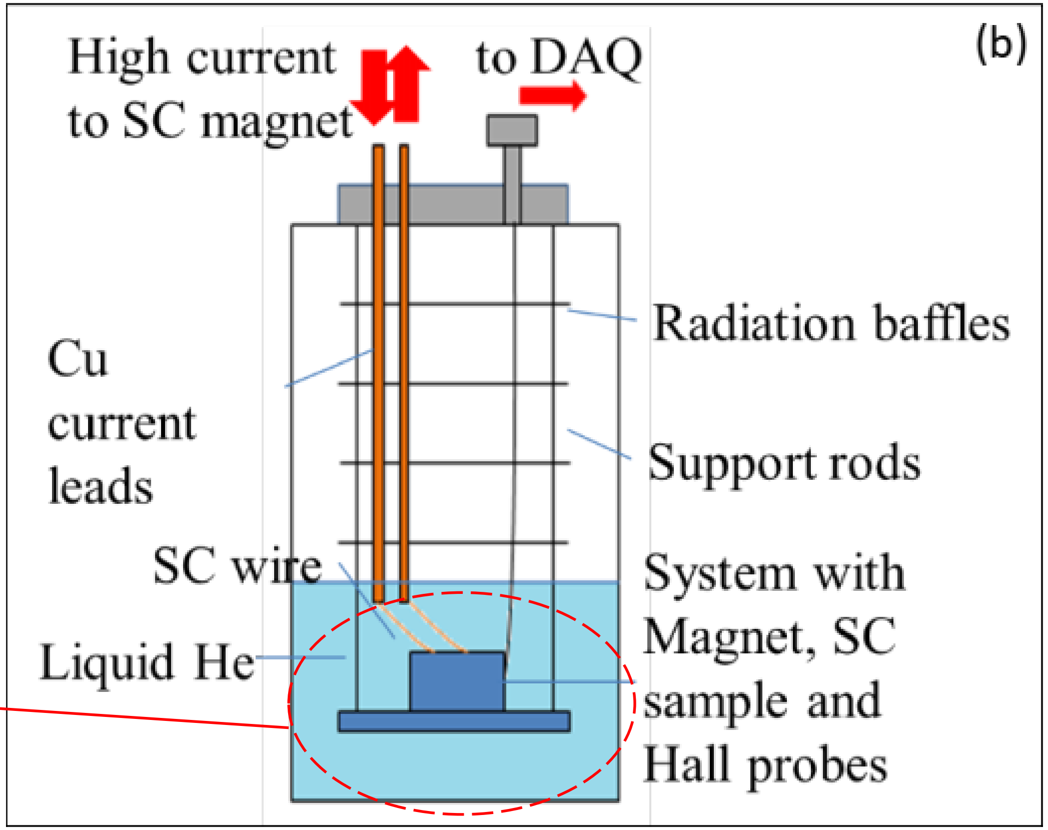
(b)
High current to SC magnet
to DAQ
Radiation baffles
Cu current leads
Support rods
SC wire
System with Magnet, SC sample and Hall probes
Liquid He

# Magnet Fabrication

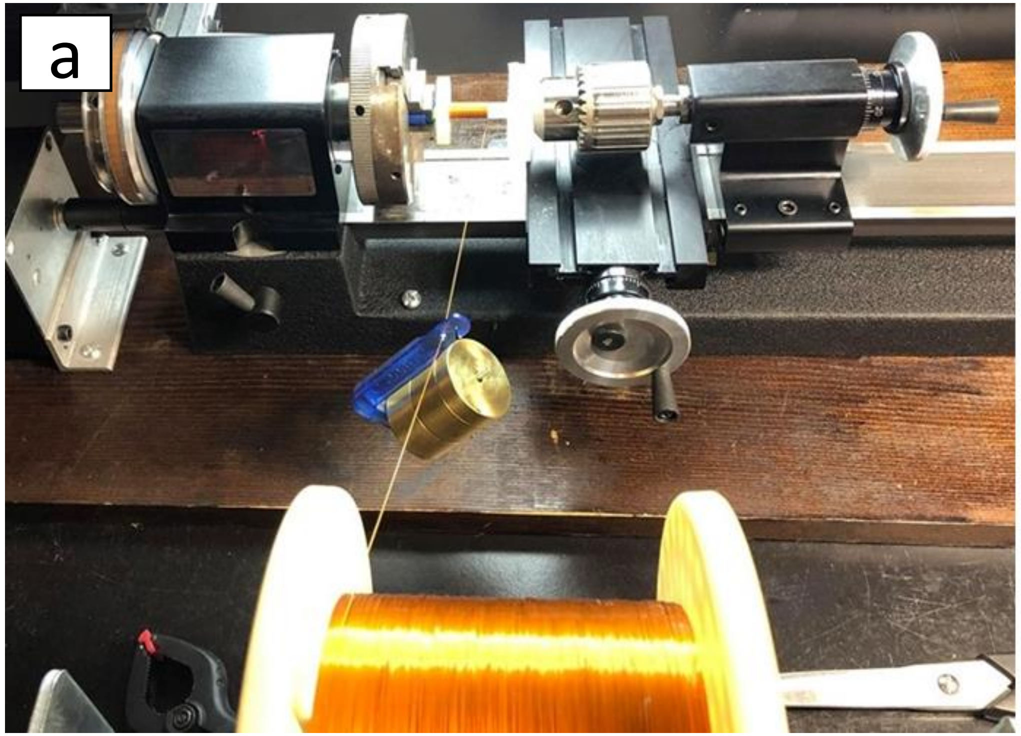


Magnet winding set up

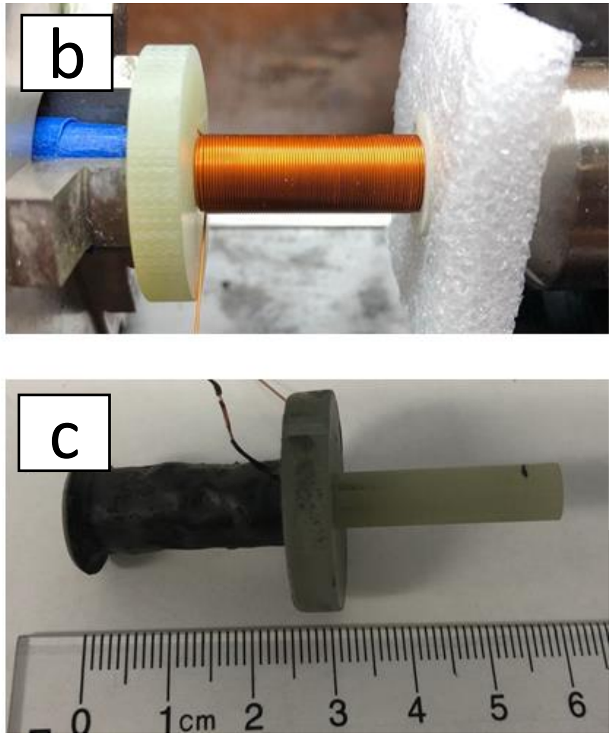


Magnet covered with epoxy

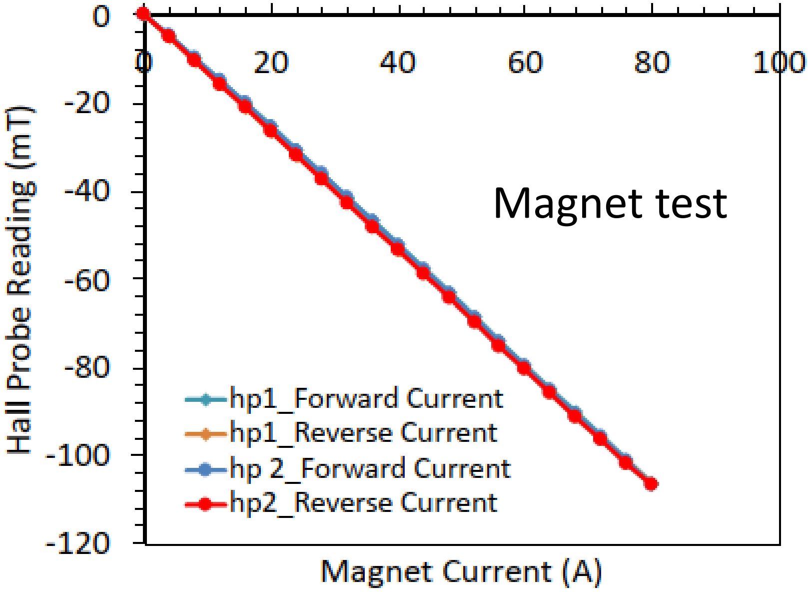


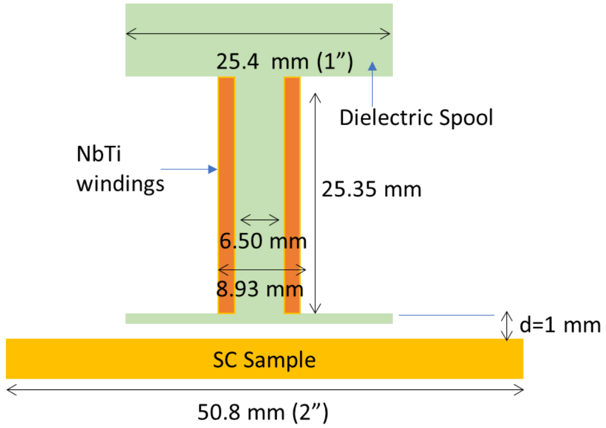


NbTi SC magnet allows to apply high current more than 80 A in order to have high field at the sample surface greater than 500 mT

# Hall Probes used in the setup

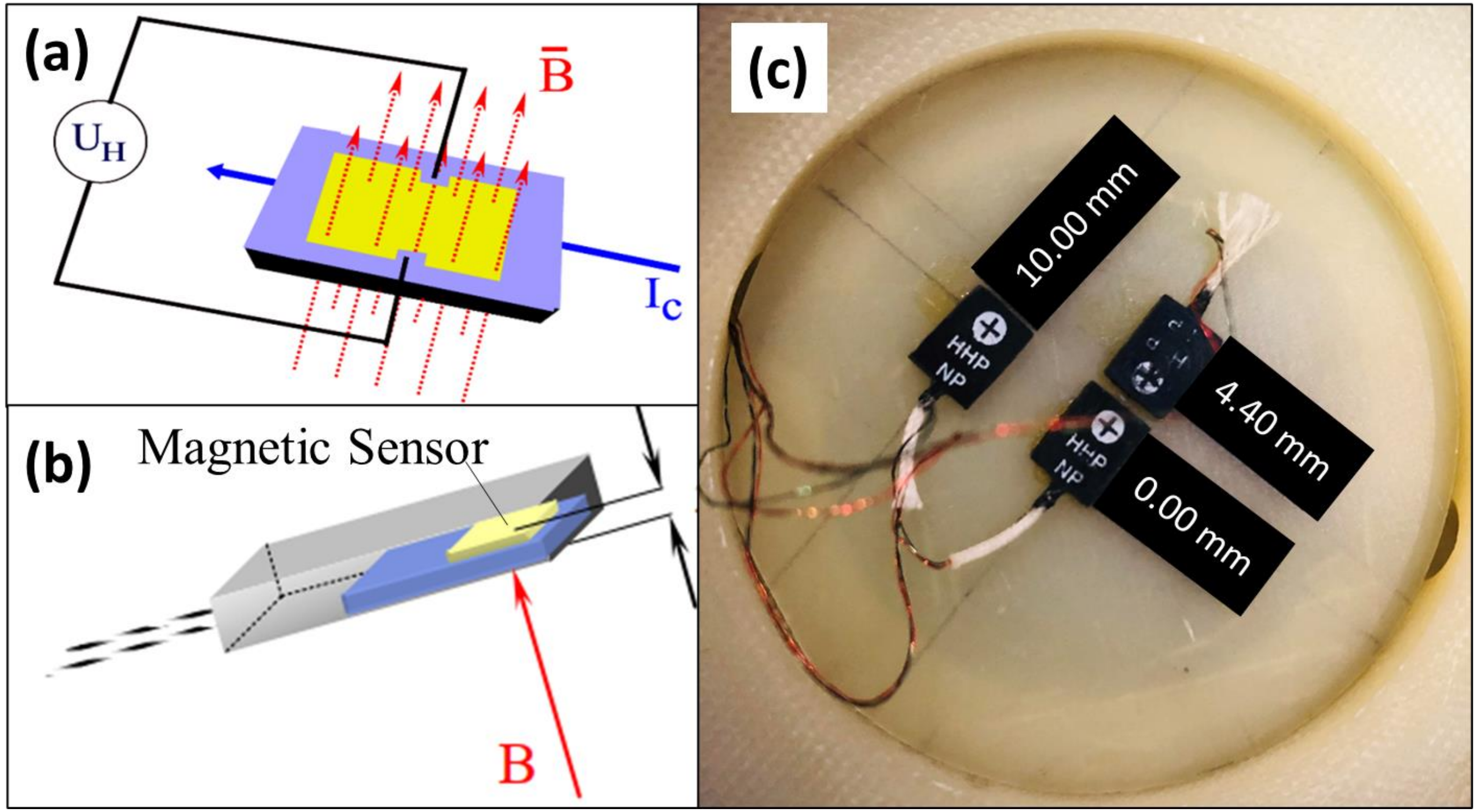


(a) HHP-NP Hall probes used in the experimental setup that can detect the component of the magnetic field perpendicular to the probe

(b) the Hall sensor located inside the probe covered with the resin

(c) configuration of the Hall probes mounted at the bottom of the sample

# Setup Calibration: Method 1

Thickness of the samples ≈100 µm

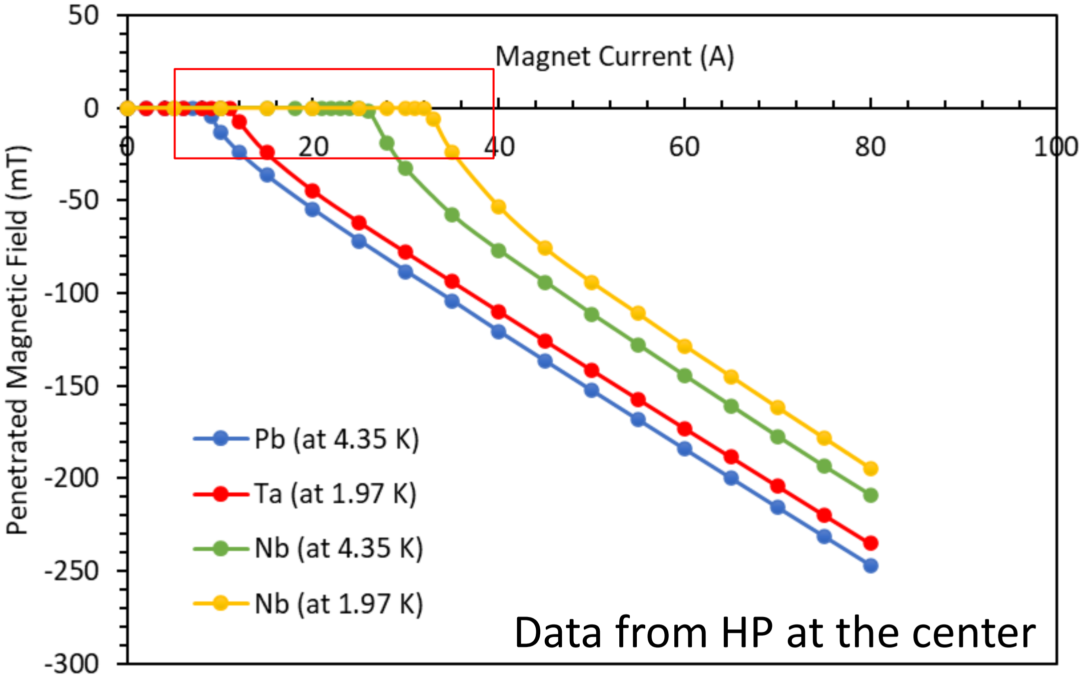


Calibration Curve

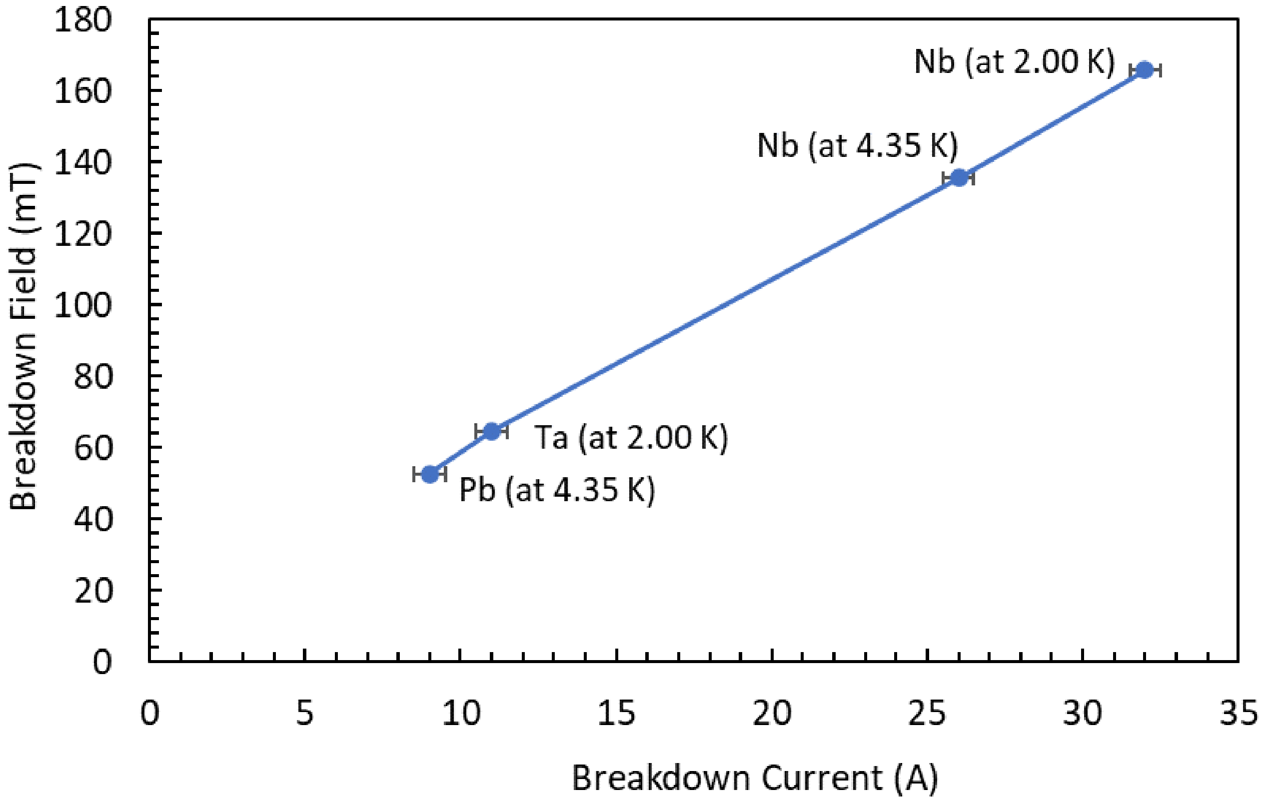


Ref:

- G. Chanin and J. P. Torre, "Critical-field curve of superconducting lead," Phys. Rev. B **5**, 4357–4364 (1972).
- D. K. Finnemore, T. F. Stromberg, and C. A. Swenson, "Superconducting properties of high-purity niobium," Phys. Rev. **149**, 231–243 (1966)
- C. H. Hinrichs, C. A. Swenson, "Superconducting critical field of tantalum as a function of temperature and pressure", *Phy. Rev.* Vol. 123, No. 4, 1961

# Setup Calibration: Method 2

Measurements of $B_z$ with increasing magnet current

**(a) Test 1**

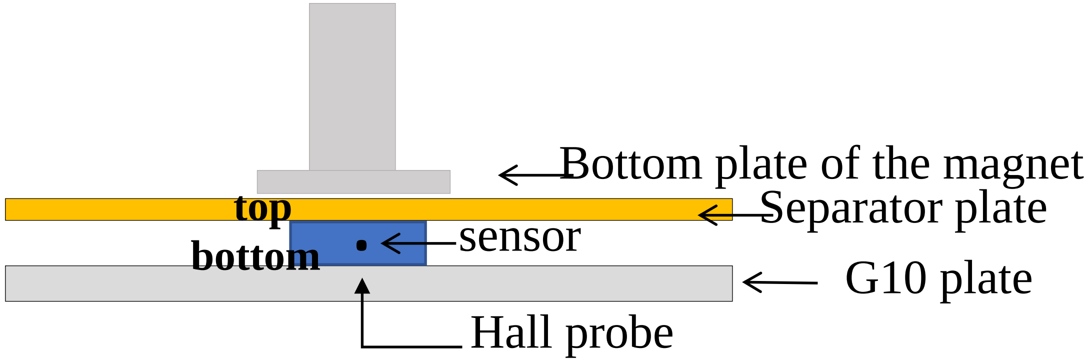


**(b) Test 2**

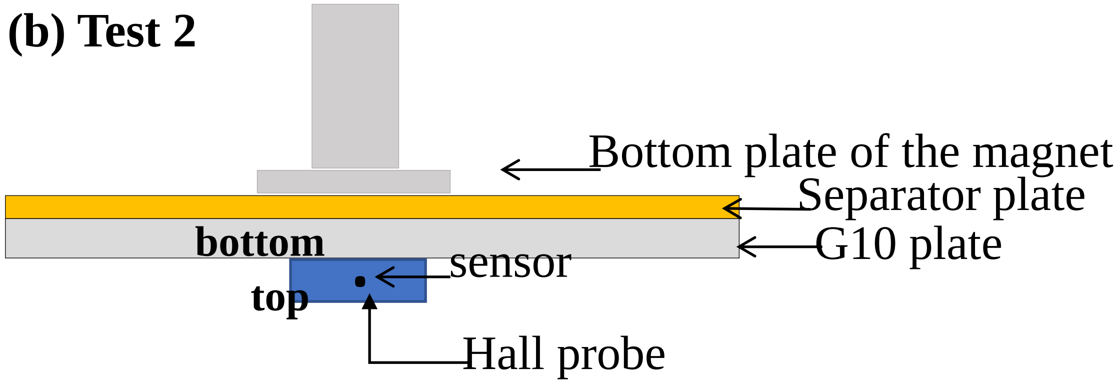


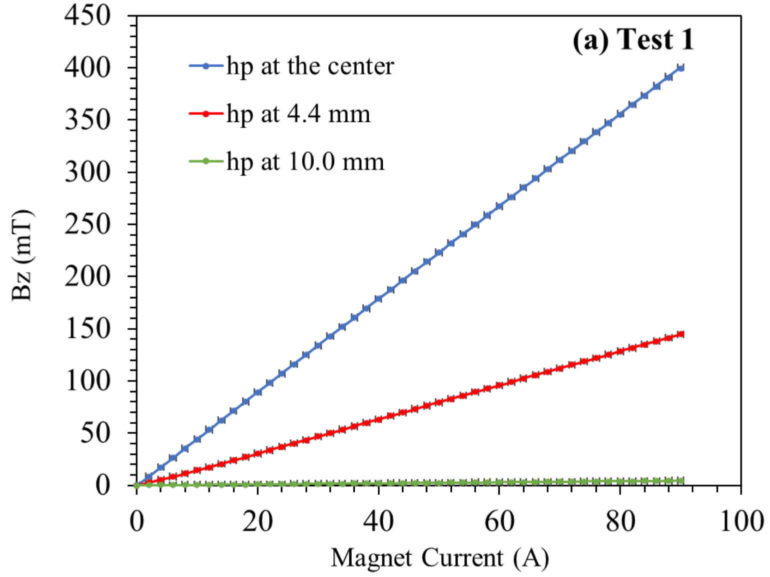


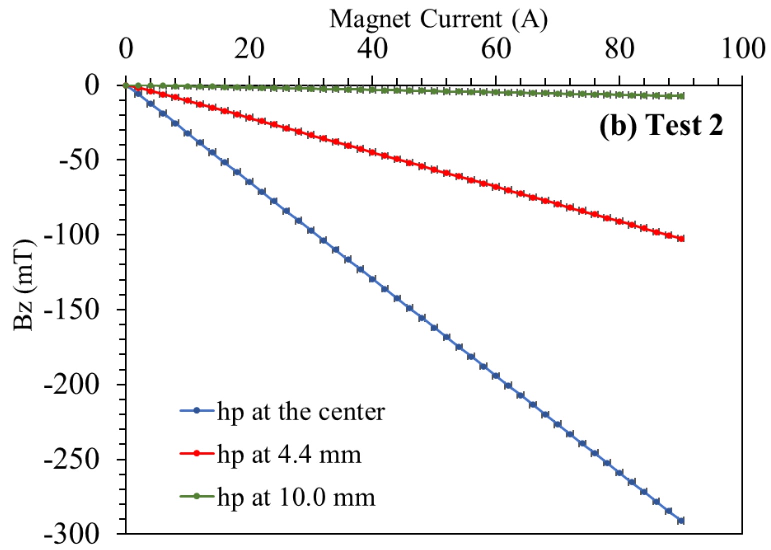

## Test 01

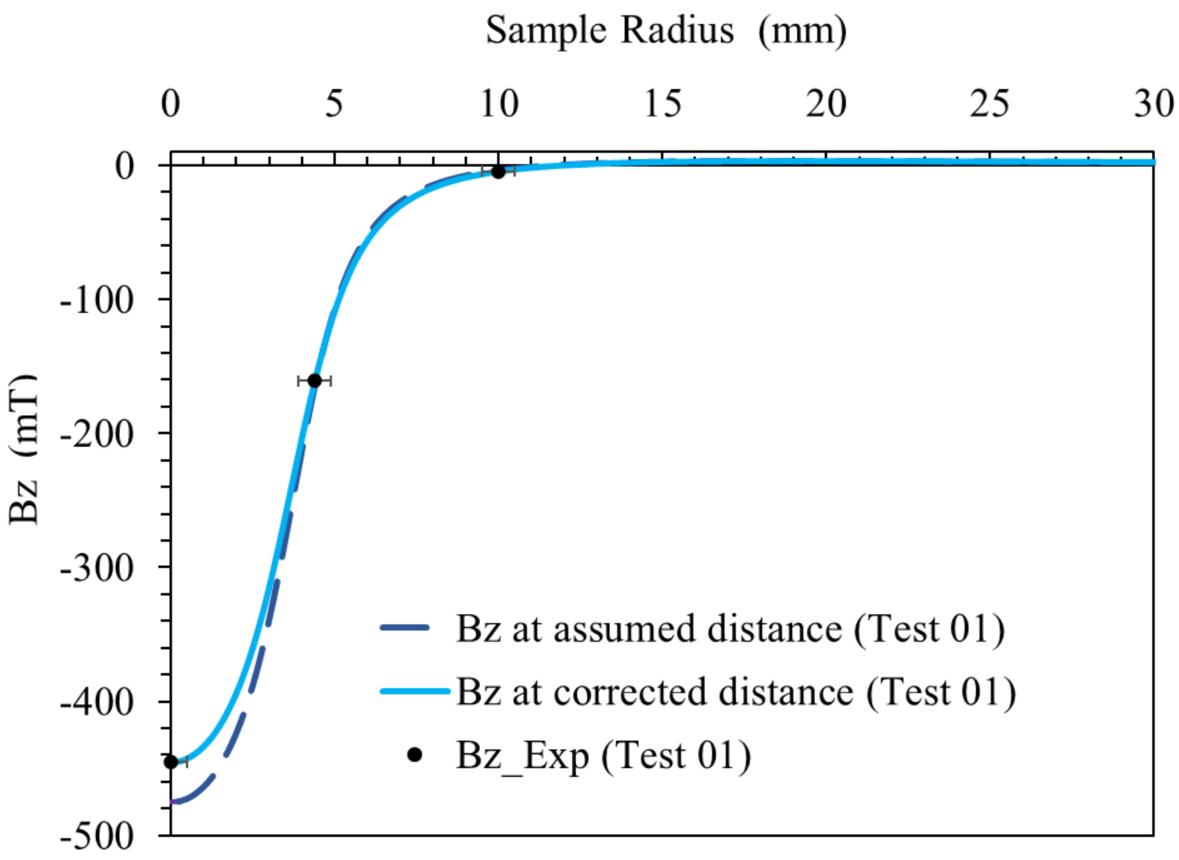


## Test 02

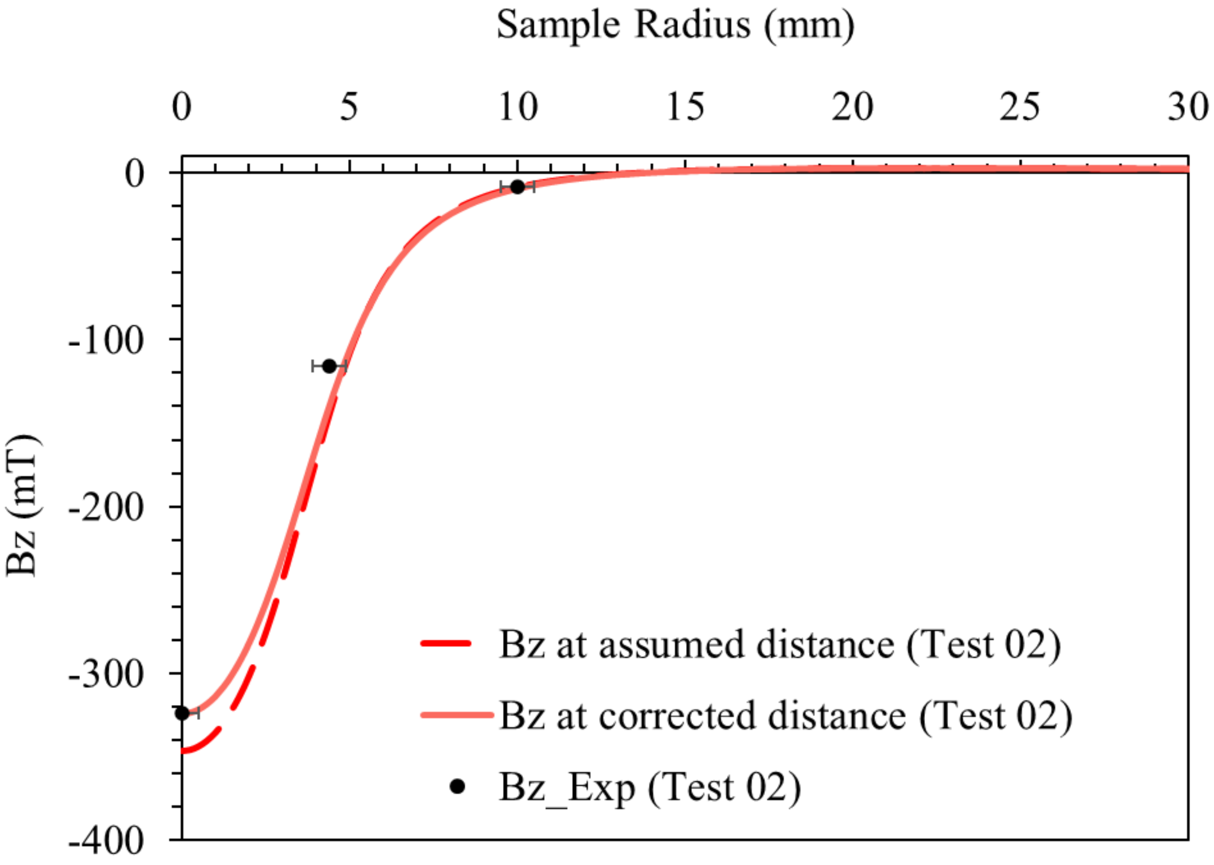


**Corrected-Assumed = 0.19 mm < less than magnet wire**

# Calibrated Magnetic field on the surface in Meisnner state at 100 A of current

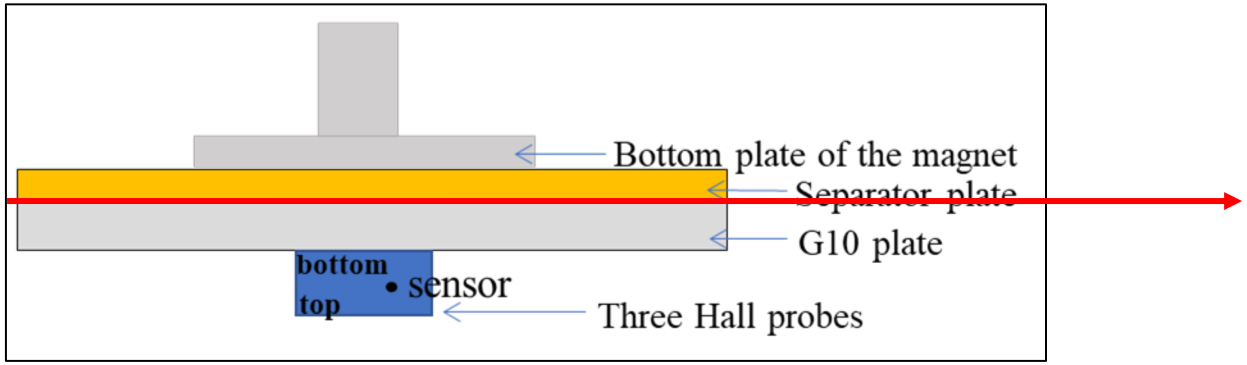


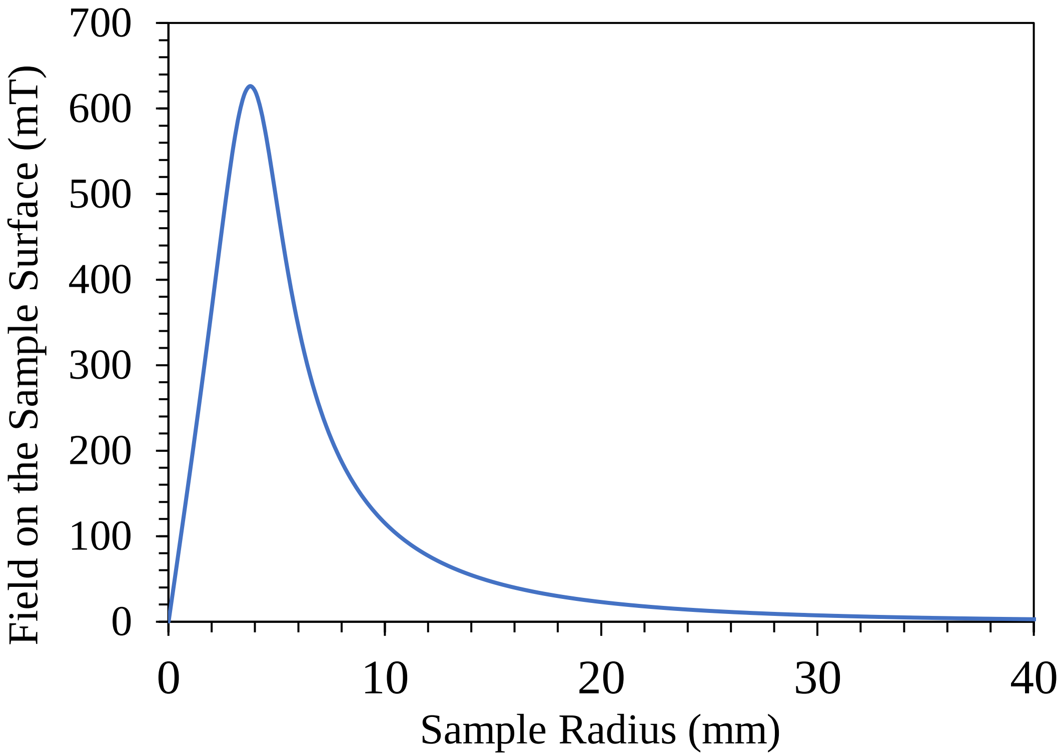


Corrected separation between magnet and sample surface= 0.992+0.19=**1.182 mm**

**Maximum magnetic field at 100 A = 626 mT**

**Maximum magnetic field = 6.26 mT/A** → Used to current – field conversion, but only valid up to breakdown field

# 1-Measurements on Bulk Superconductors

# Lead (Pb) and Niobium (Nb)

Thickness of the samples ≈250 µm

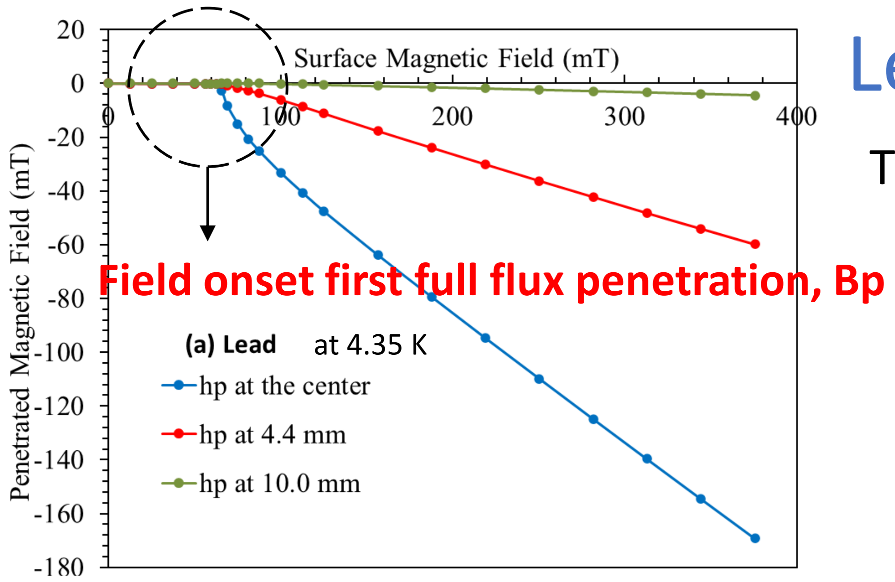


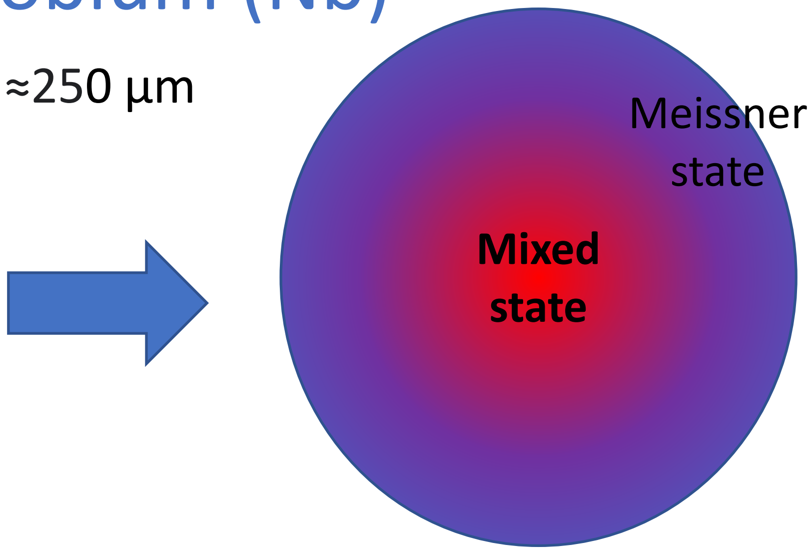


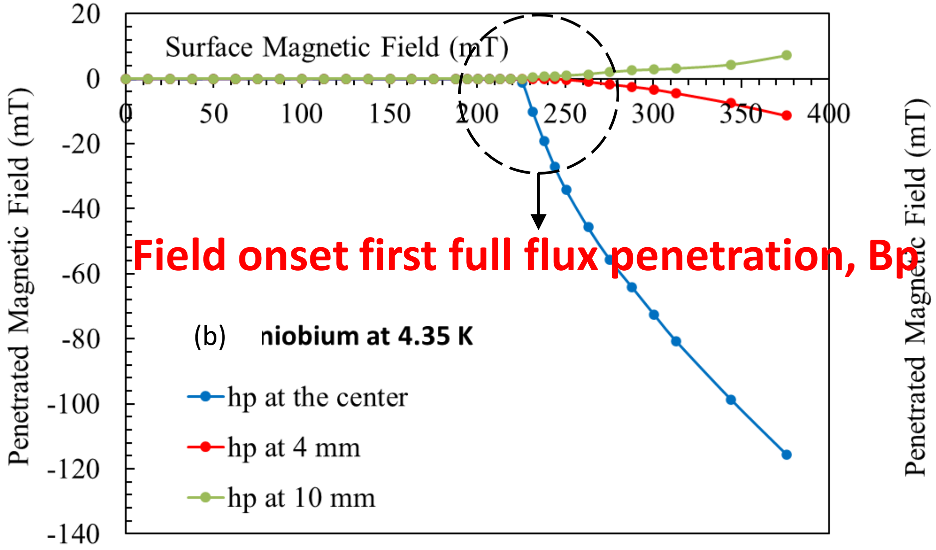


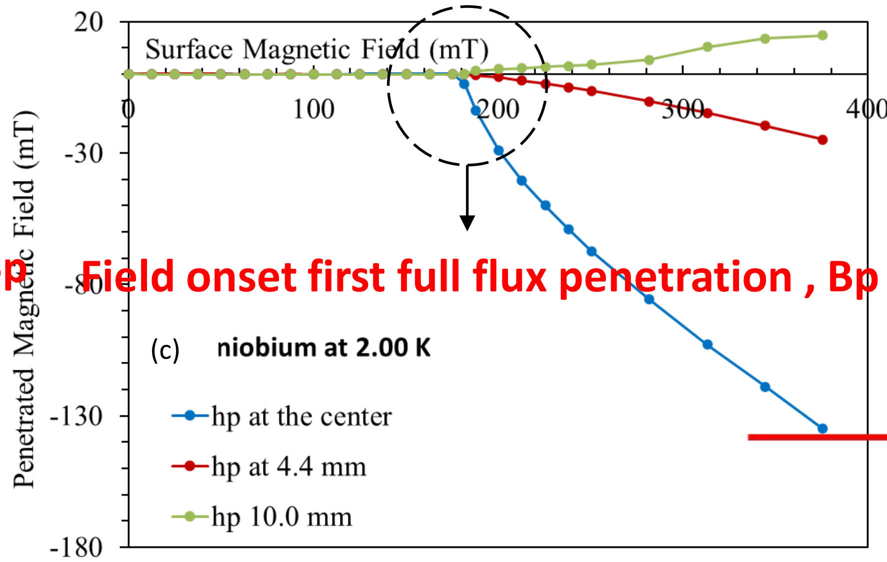


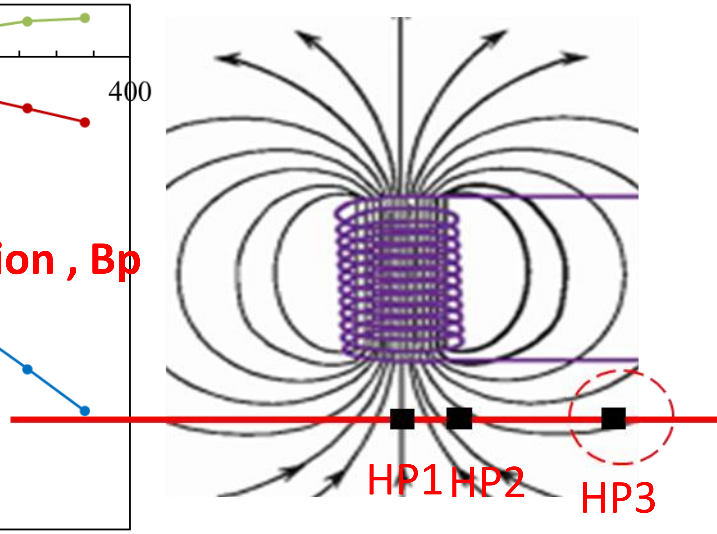

# Thickness Effect

## Lead (Pb)

### At 4.35 K

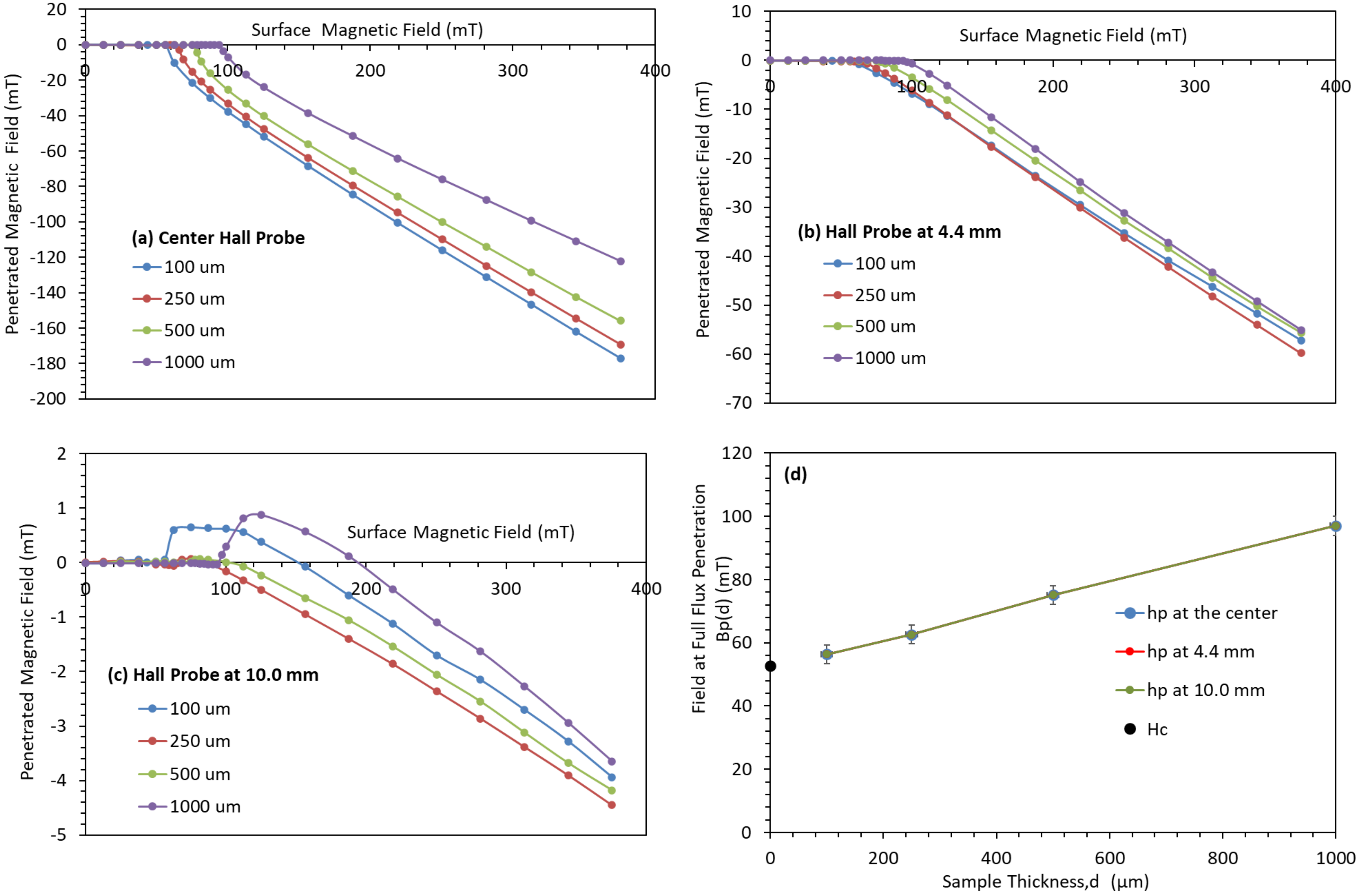


| Hc (mT) at 4.35 K | |
|---|---|
| Extrapolated | 51.29 |
| From Ref | 52.64 |

Ref: G. Chanin and J. P. Torre, "Critical-field curve of superconducting lead," Phys. Rev. B **5**, 4357–4364 (1972).

# Thickness Effect

## Niobium (Nb) at 4.35 K and 2.00 K

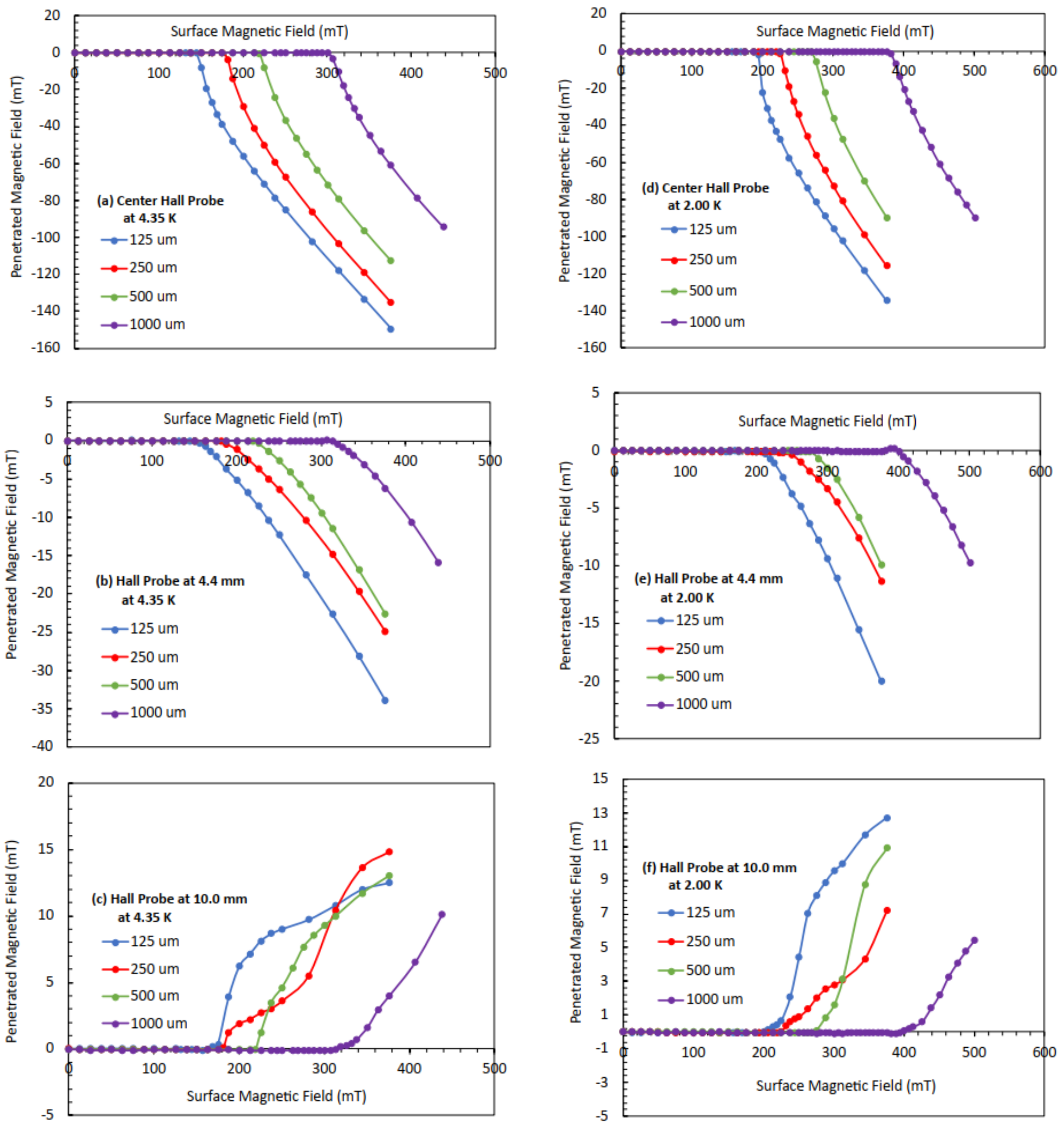


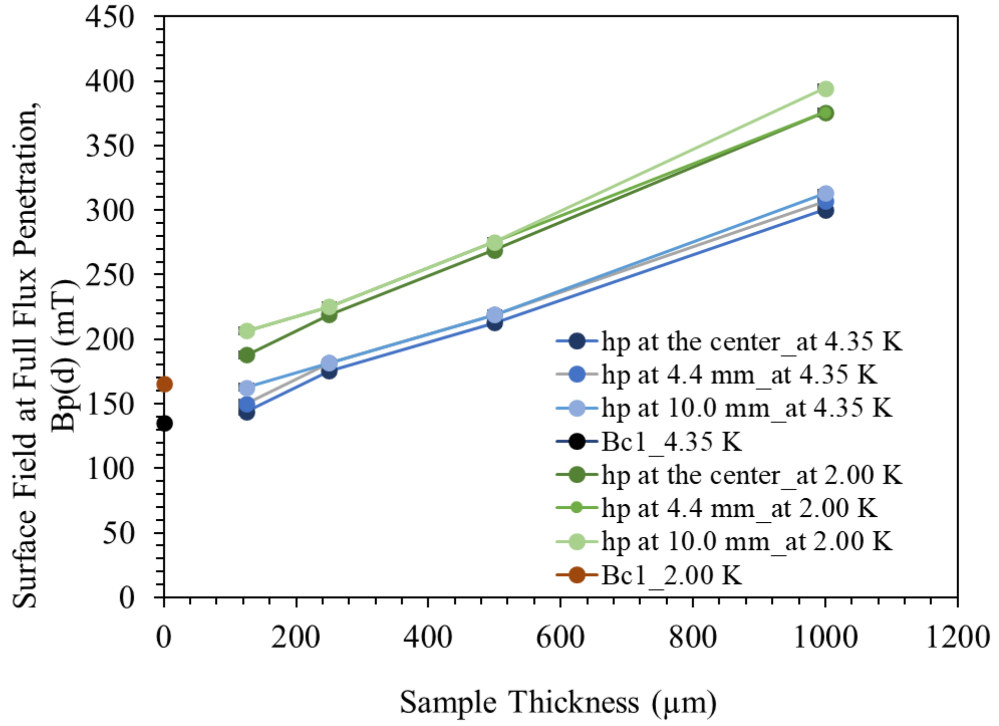


| Hc1 (mT) | 4.35 K | 2.00 K |
|---|---|---|
| Extrpolated | 132.54 | 163. 30 |
| From Ref | 135.52 | 165.86 |

Ref: D. K. Finnemore, T. F. Stromberg, and C. A. Swenson, “Superconducting properties of high-purity niobium,” Phys. Rev. **149**, 231–243 (1966)

# Conclusions

- MFP Magnetometer has been developed to detect the field onset of magnetic flux penetration, $B_p$ through flat samples of SRF materials.

- Testing the setup on Pb and Nb bulk samples was successful. The variation of $B_p$ is linear with the thickness of sample and it has reproduced the well-known values of critical magnetic fields of these materials.

# 2-Measurements on Thin Film Superconductors

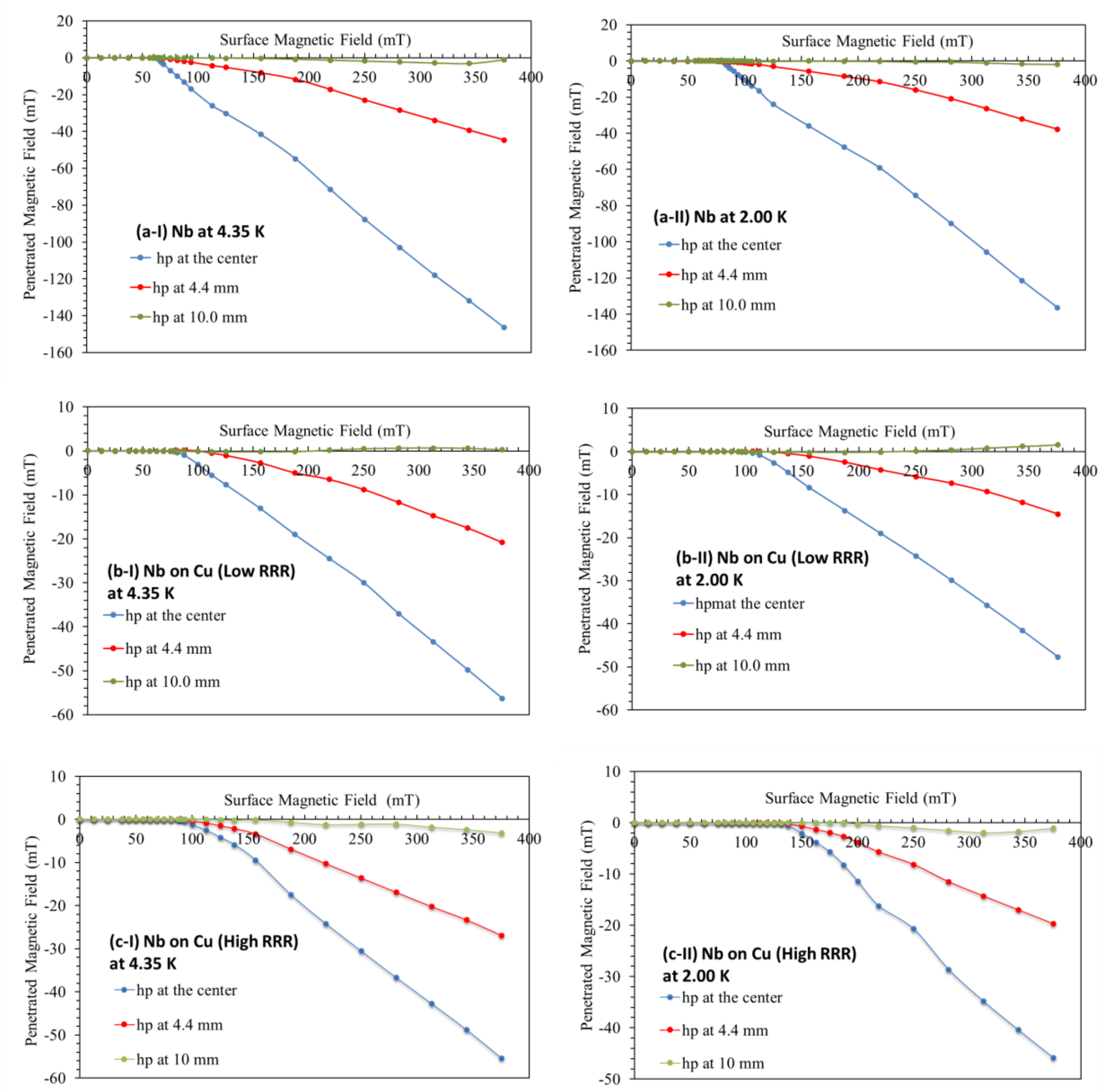


Magnetic Feld Penetration Measurements on **Nb thin film** by Electron Cyclotron Resonance (ECR) at Jefferson Lab.

Thickness of the films ~1-3 µm

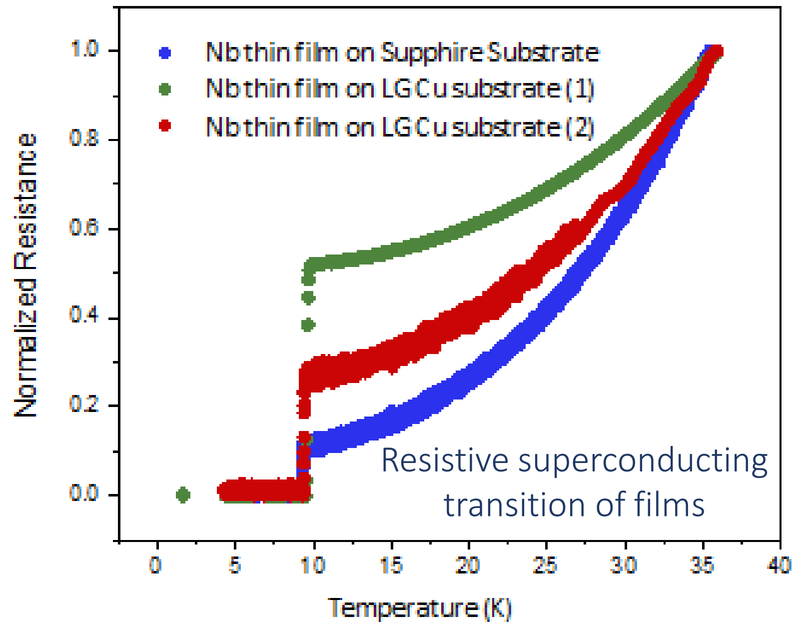


| Sample | RRR | Tc | ΔTc | Bp (mT) | |
|---|---|---|---|---|---|
| | | | | 4.35 K | 2.00 K |
| Nb on Sapphire | 332 | 9.31 | 0.03 | 62.6 | 80.1 |
| Nb on LGCu (1) | 34 | 9.57 | 0.28 | 78.3 | 97.0 |
| Nb on LGCu (2) | 190 | 9.47 | 0.24 | 90.8 | 125.2 |

1.5 $\mu$m thick **$Nb_3Sn$ thin film** grown on sapphire wafer by multilayer sequential sputtering at room temperature and annealed at 950 °C at Jefferson Lab.

| $Nb_3Sn$ Critical Fields | |
|---|---|
| $H_{c1}$ (4.35 K) mT | 36 |
| $H_{sh}$ (4.35 K) mT | 414 |

XRD Analysis

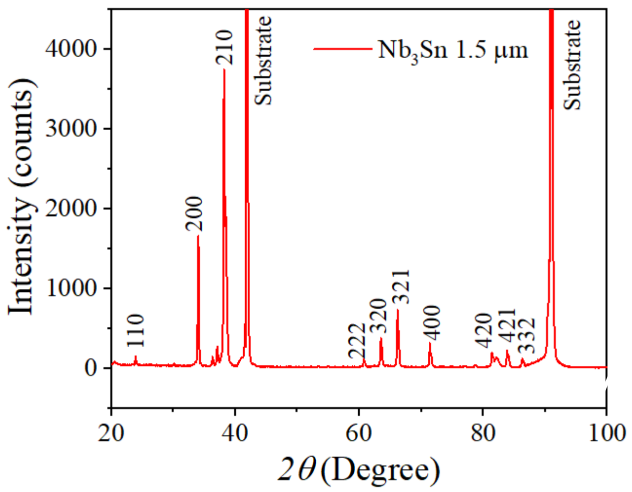


Resistive superconducting transition of film

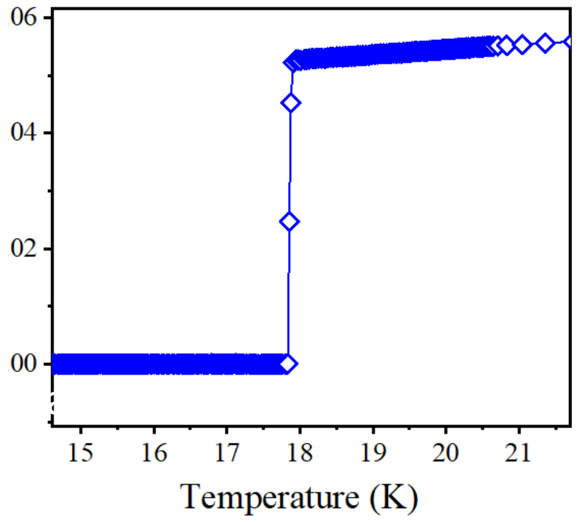


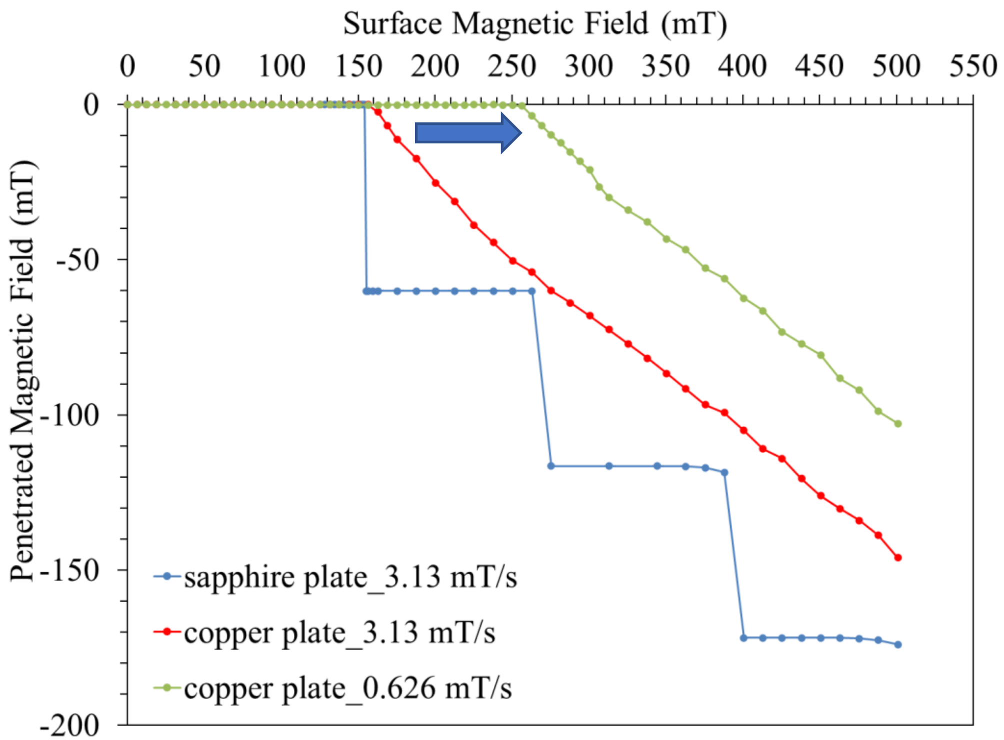


Field penetration measurements at 4.35 K

Field penetration measurements from Hall Probe at 4.4 mm and 10.0 mm at 4.35 K on 1.5 $\mu$m thick $Nb_3Sn$ thin film grown on $Al_2O_3$ wafer by multilayer sequential sputtering at room temperature and annealed at 950 $^oC$ at Jefferson Lab.

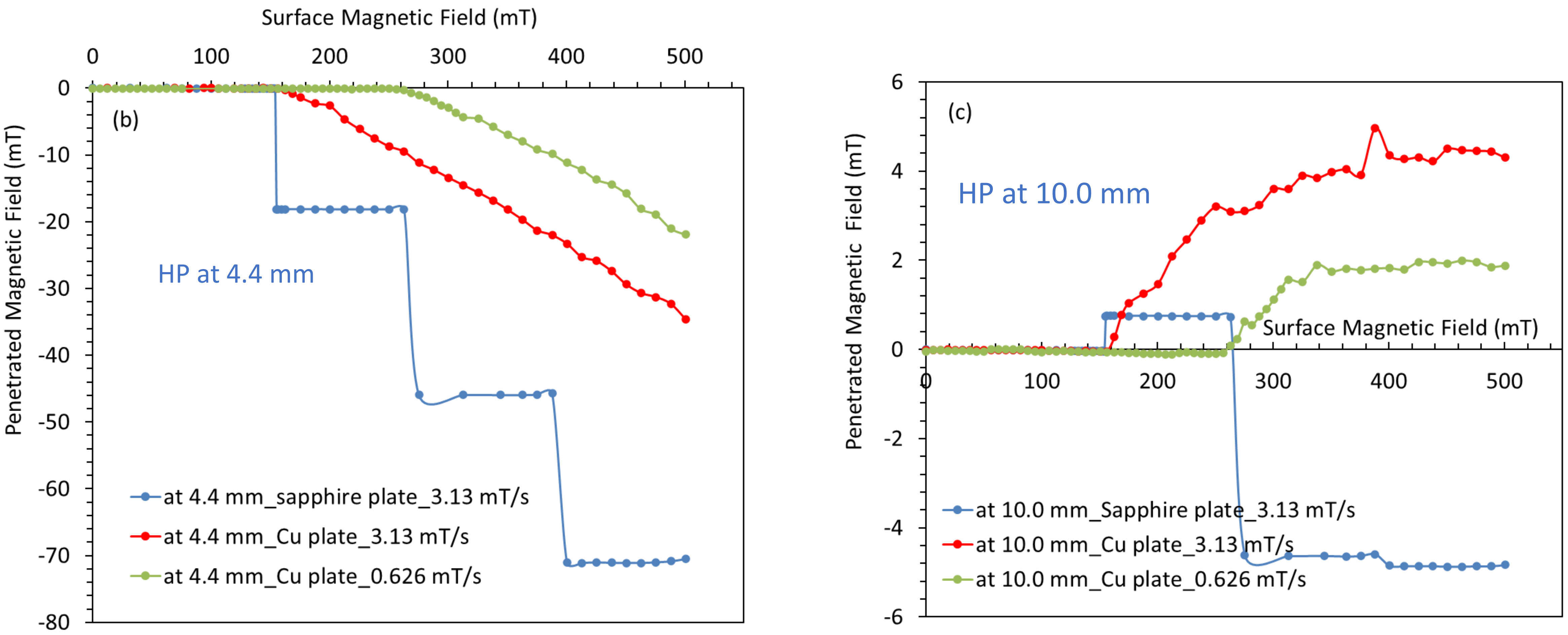

**$Nb_3Sn/Al_2O_3$ multilayer** grown on sapphire wafer by high-temperature confocal sputtering at the University of Wisconsin-Madison. This multilayer sample consists of four 60 nm $Nb_3Sn$ layers separated by 6 nm $Al_2O_3$ interlayers.

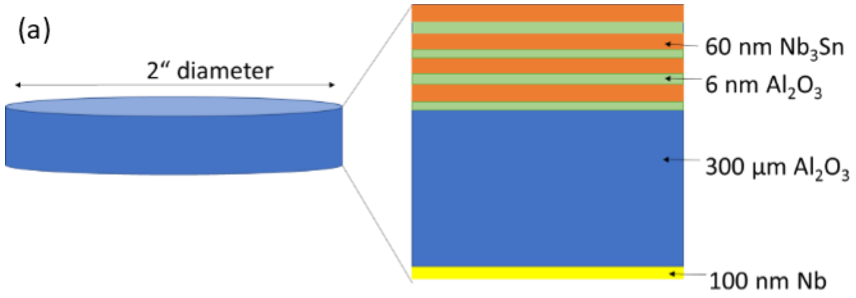


Schematic of $Nb_3Sn/Al_2O_3$ multilayer heterostructures on $Al_2O_3$ wafer. Back side of $Al_2O_3$ wafer is coated with a thick Nb film.

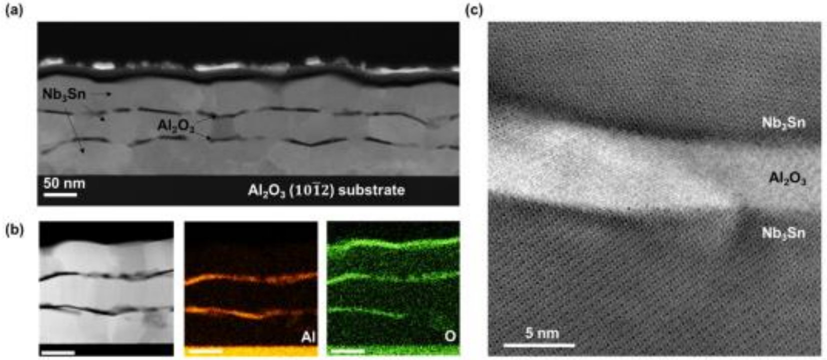


Cross-sectional transmission electron microscopy images of $Nb_3Sn/Al_2O_3$ multilayer heterostructures

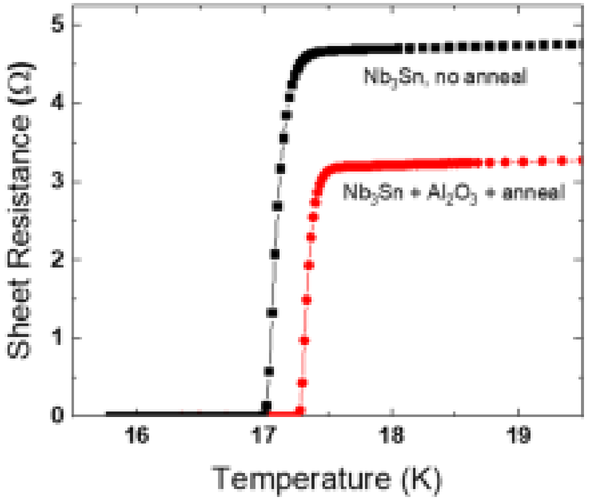


Resistive superconducting transition

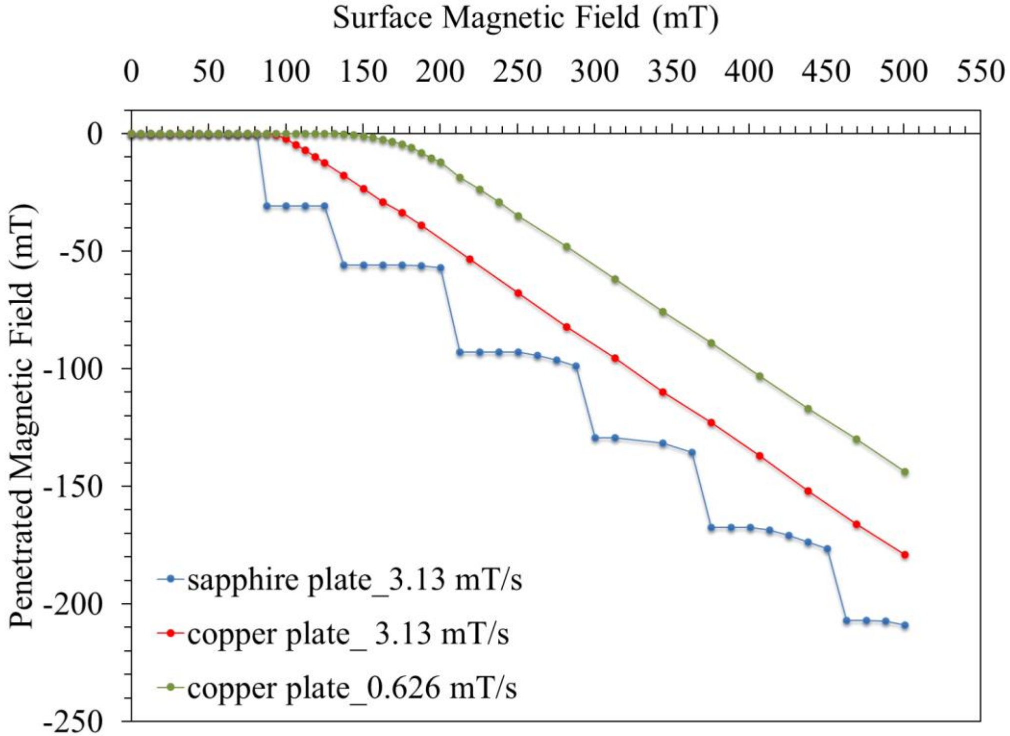


Sundahl *et al* , **Sci. Rep. 11, 7770 (2021)**

Magnetic Feld Penetration Measurements

Magnetic Feld Penetration Measurements Hall Probe at 4.4 mm and 10.0 mm at 4.35 K on $Nb_3Sn/Al_2O_3$ multilayer grown on $Al_2O_3$ wafer by high-temperature confocal sputtering at the University of Wisconsin-Madison. This multilayer sample consists of four 60 nm $Nb_3Sn$ layers separated by 6 nm $Al_2O_3$ interlayers.

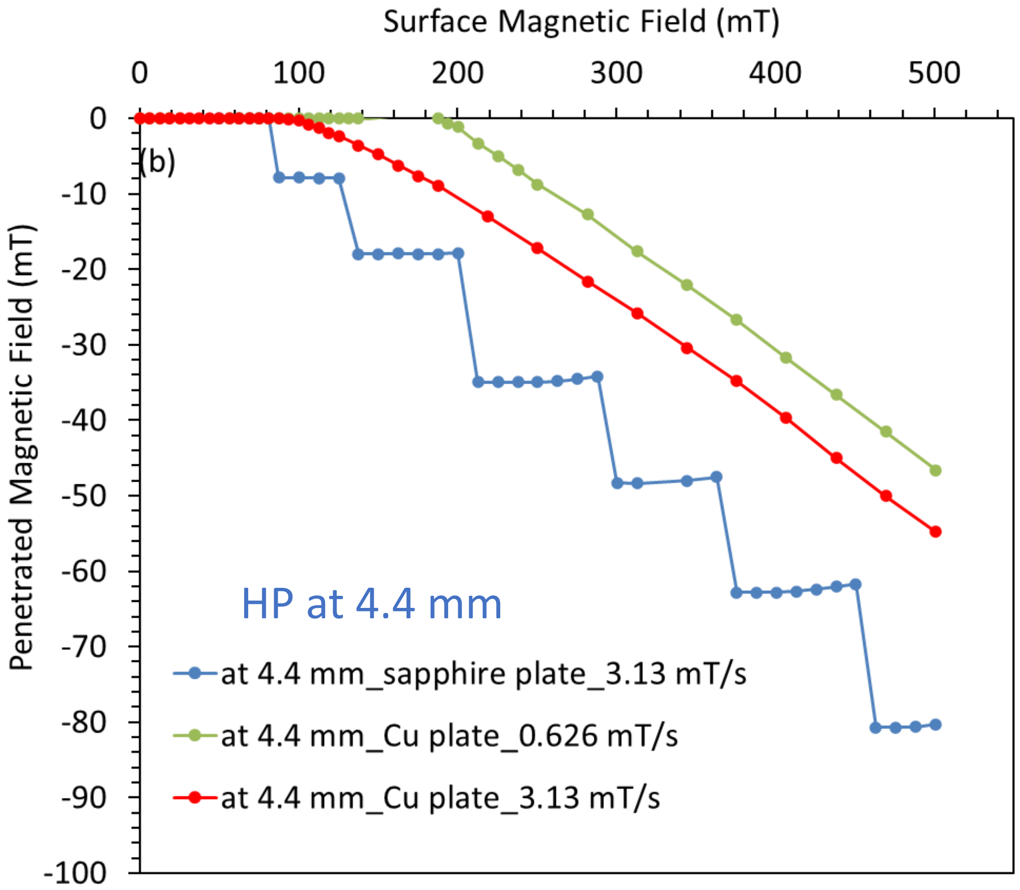


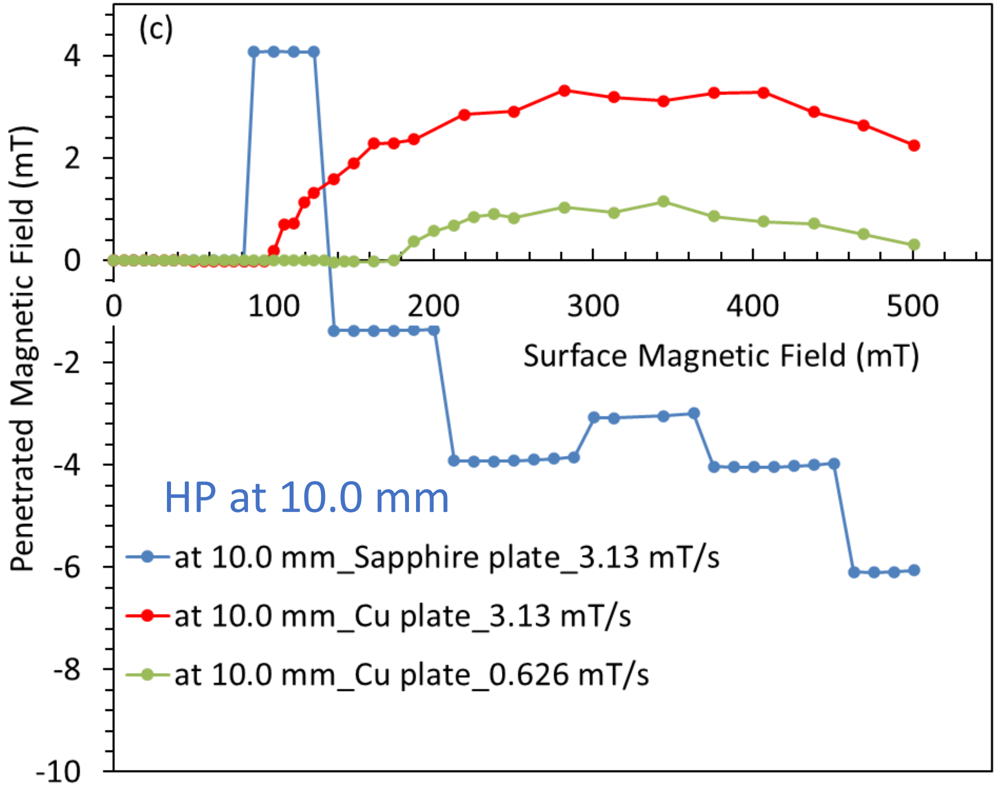

# Conclusions

- Thin film measurements of Bp using MFP magnetometer was successful and this is a nondestructive technique for thin film measurements.
- The dependent of Bp with material purity was observed using Nb thin films coated on Cu substrates.
- Low conductive thin film materials, such as $Nb_3Sn$ films, and multilayers exhibit flux jumps due to thermomagnetic flux avalanches. These flux jumps were mitigated by improving heat transfer across the sample and slowing down the magnet ramp rate.

# 3-Measurements on Multilayered Niobium

- NbTiN and AlN thin layers are deposited on bulk Nb using reactive Direct Current Magnetron Sputtering (reDCMS) in an Ultra-High Vacuum (UHV) system with a base pressure of $10^{-10}$Torr.
- The Nb substrates are prepared by buffered chemical polishing (BCP) removing 5um from the surface.
- The films were deposited at 450 °C on bulk Nb after a 24 hour bake at 600 °C, then post-annealed at 450 °C for 4 hours.

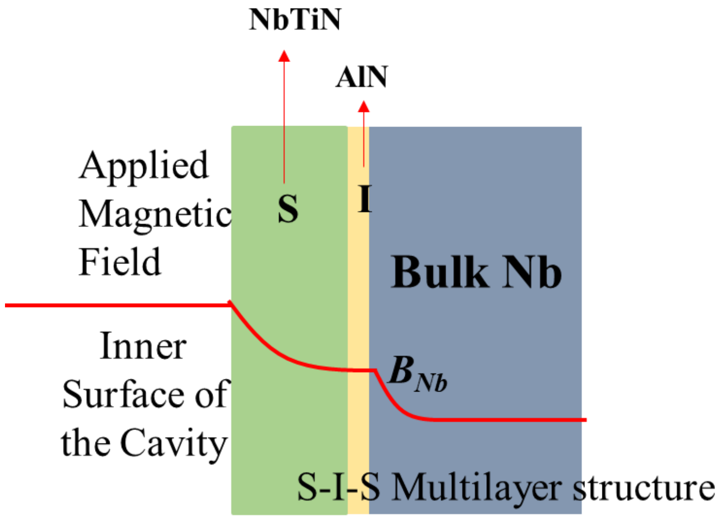


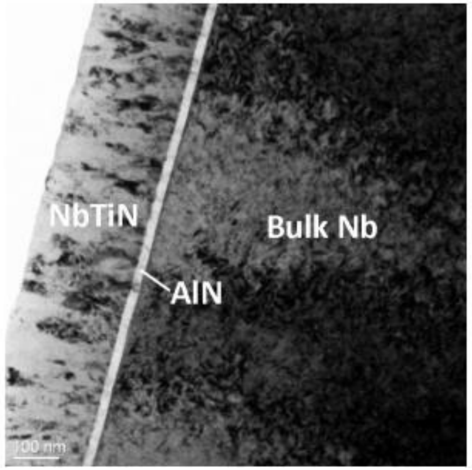


Cross-sectional transmission electron microscopy image of NbTiN/AlN/Nb structure
A.-M. Valente-Feliciano et al, SRF2013

| Sample # | Thickness (nm) | |
|---|---|---|
| | NbTiN | AlN |
| 1 | 75 | 0 |
| 2 | 149 | 0 |
| 3 | 83 | ~10 |
| 4 | 166 | ~10 |
| 5 | 250 | ~10 |
| 6 | 371 | ~10 |

# Resistance measurements done by standard four-point probe method

| Sample # | Thickness (nm) | | Tc (K) | ΔT (K) |
|---|---|---|---|---|
| | NbTiN | AlN | | |
| 1 | 75 | 0 | 16.2 | 0.40 |
| 2 | 149 | 0 | 16.3 | 0.30 |
| 3 | 83 | ~10 | 14.4 | 1.49 |
| 4 | 166 | ~10 | 15.7 | 0.79 |

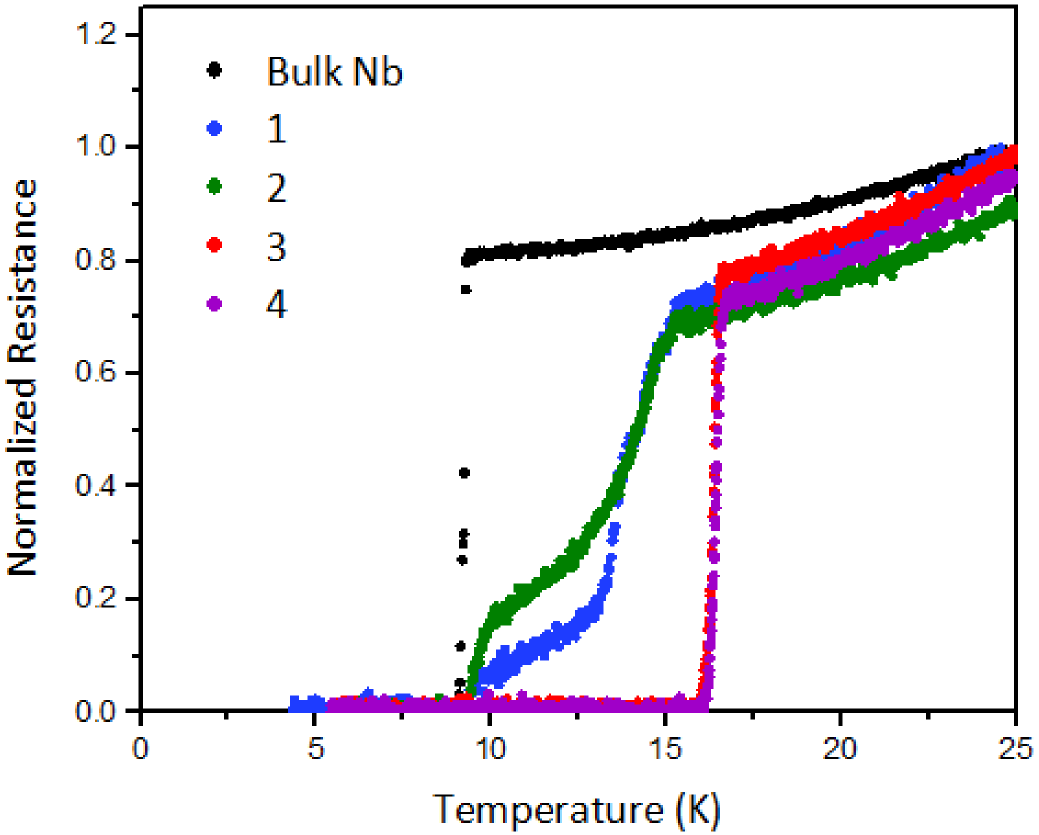

# Single layer NbTiN on Nb substrate

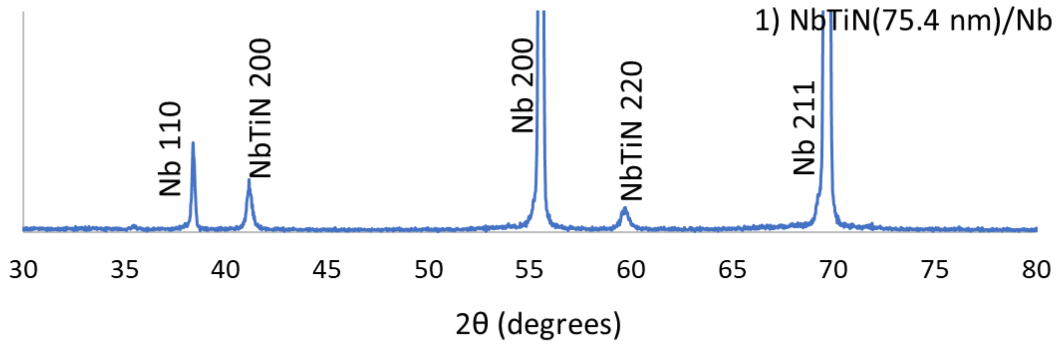


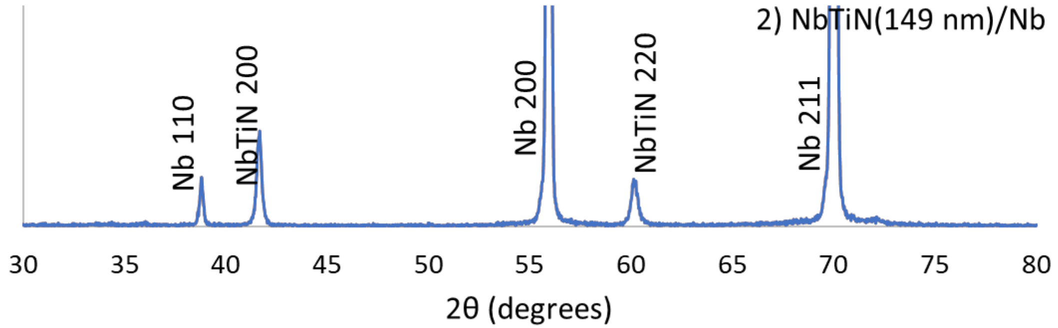


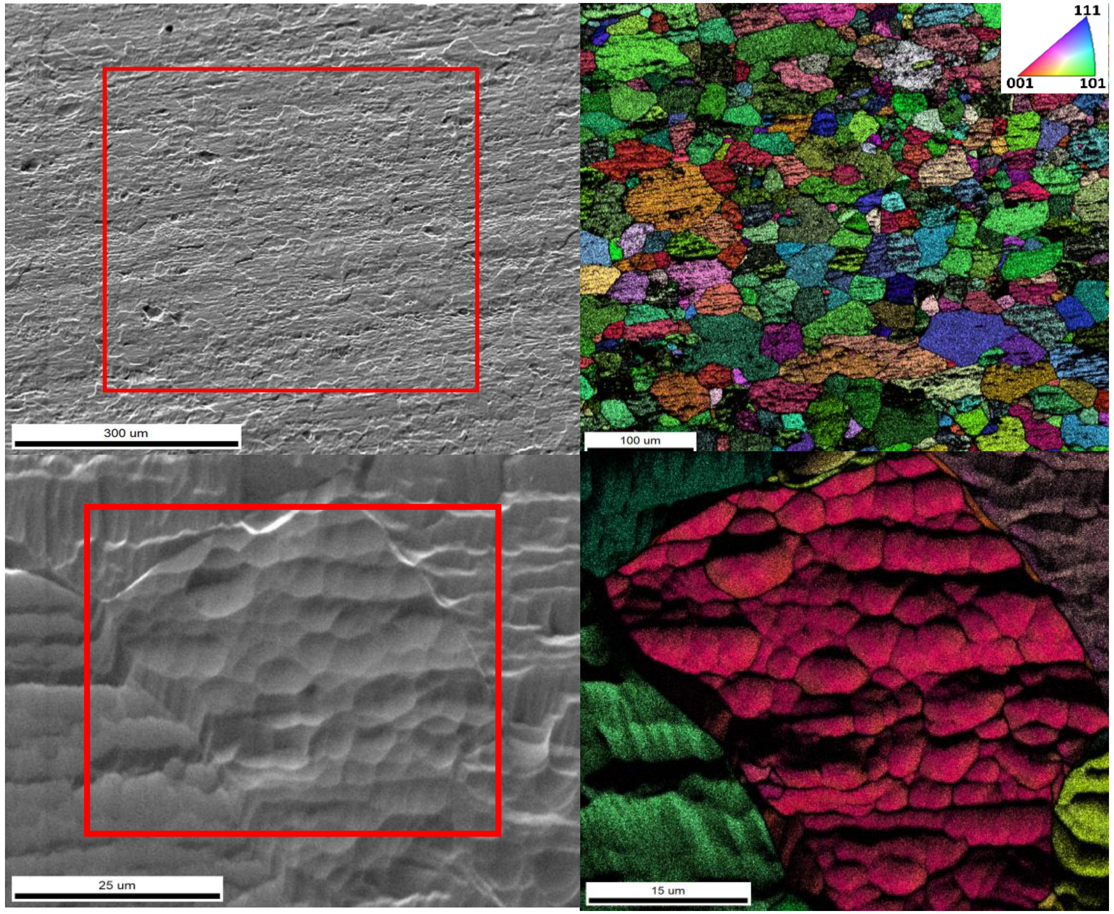


The crystallographic structures of deposited thin films were examined by X-ray diffraction (XRD) analysis

SEM images and relevant Inverse Pole Figure (IPF) map from EBSD showing the polycrystalline nature of the deposited film on bulk Nb

# NbTiN/AlN on Nb Substrate

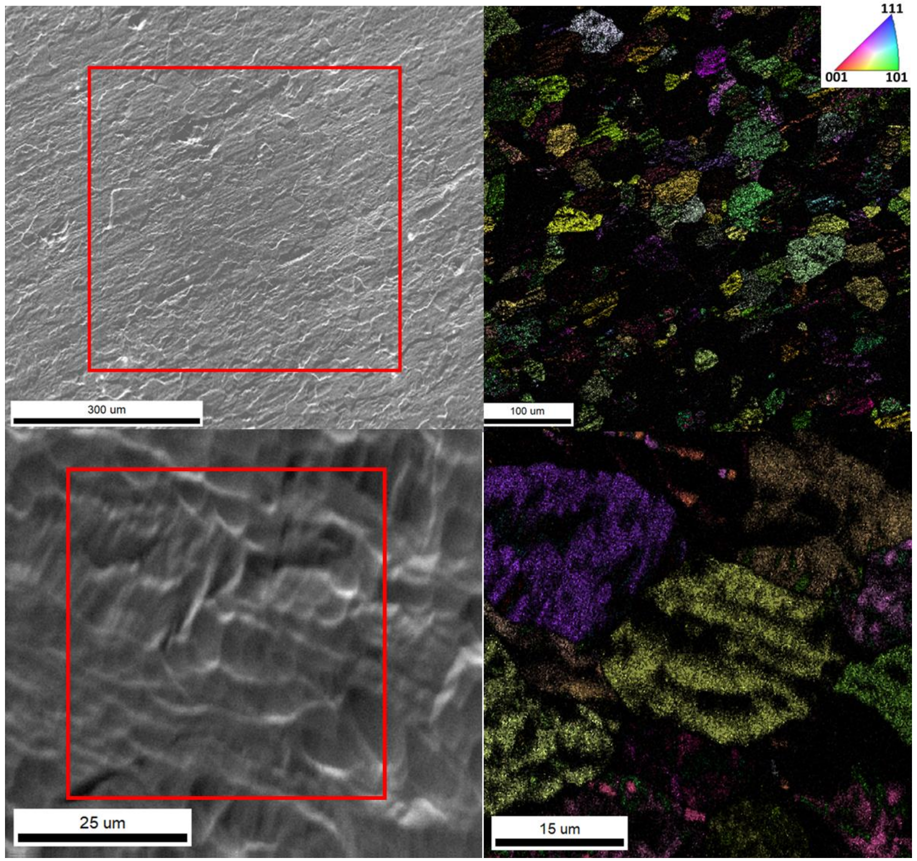


SEM images and relevant Inverse Pole Figure (IPF) map from EBSD showing the polycrystalline nature of the deposited film on bulk Nb

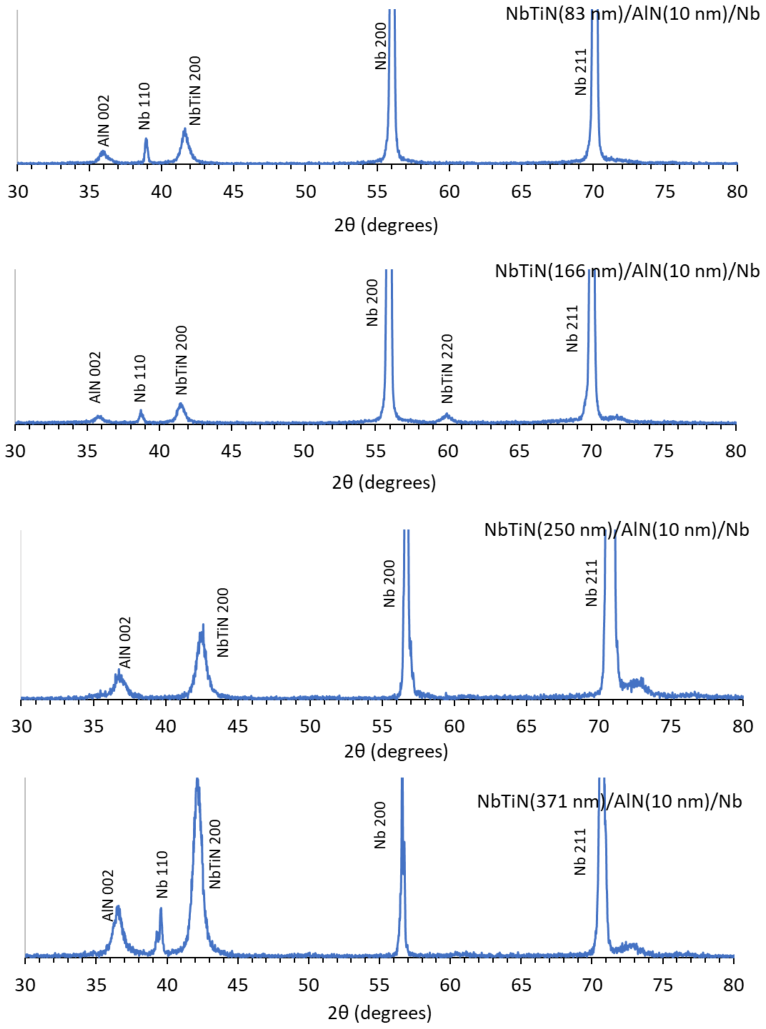


The crystallographic structures of deposited thin films were examined by X-ray diffraction (XRD) analysis

# Single layer NbTiN on Nb substrate

# Magnetic Field Penetration Measurements At 4.35 K

| Sample # | Thickness (nm) | |
|---|---|---|
| | NbTiN | AlN |
| 1 | 75 | 0 |
| 2 | 149 | 0 |

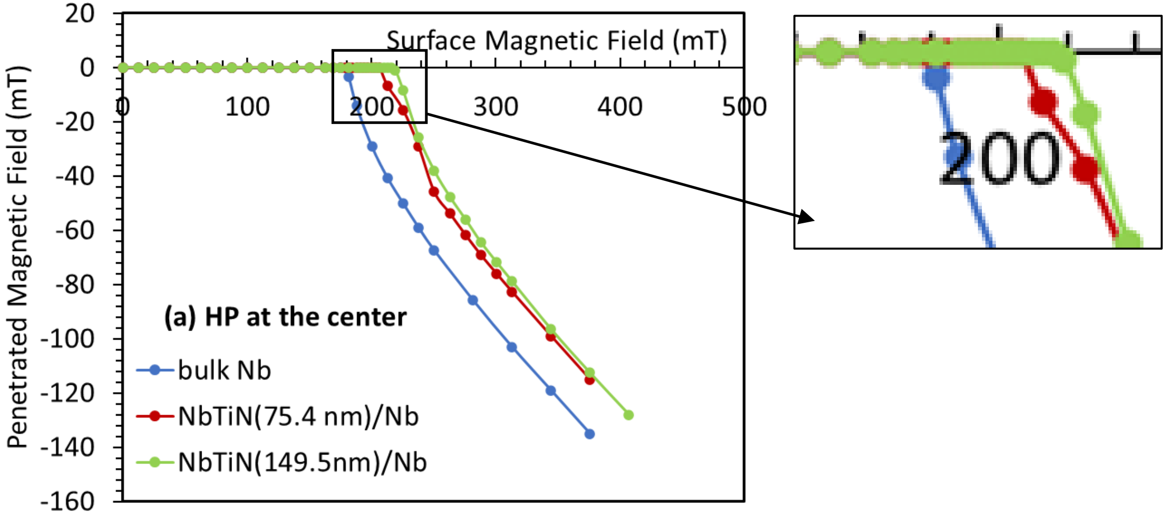


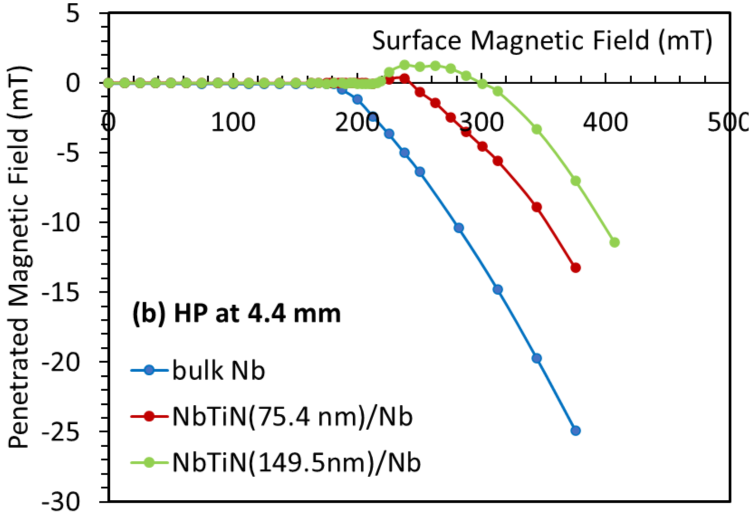


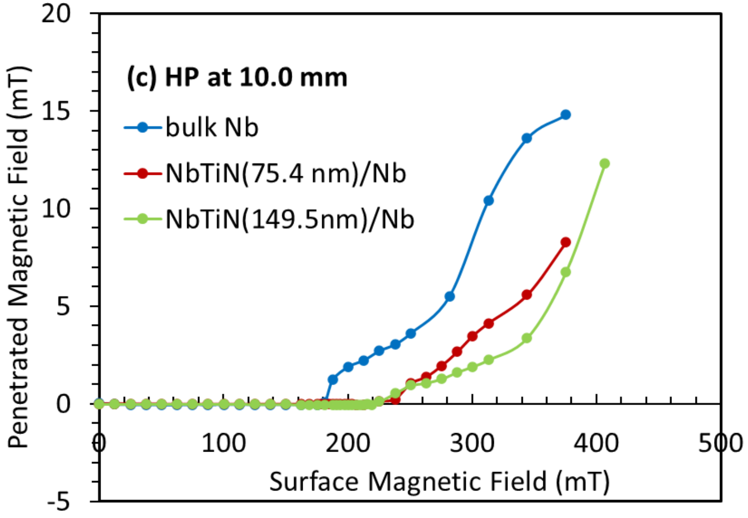

# Single layer NbTiN on Nb substrate

## Magnetic Field Penetration Measurements At 2.00 K

| Sample # | Thickness (nm) | |
|---|---|---|
| | NbTiN | AlN |
| 1 | 75 | 0 |
| 2 | 149 | 0 |

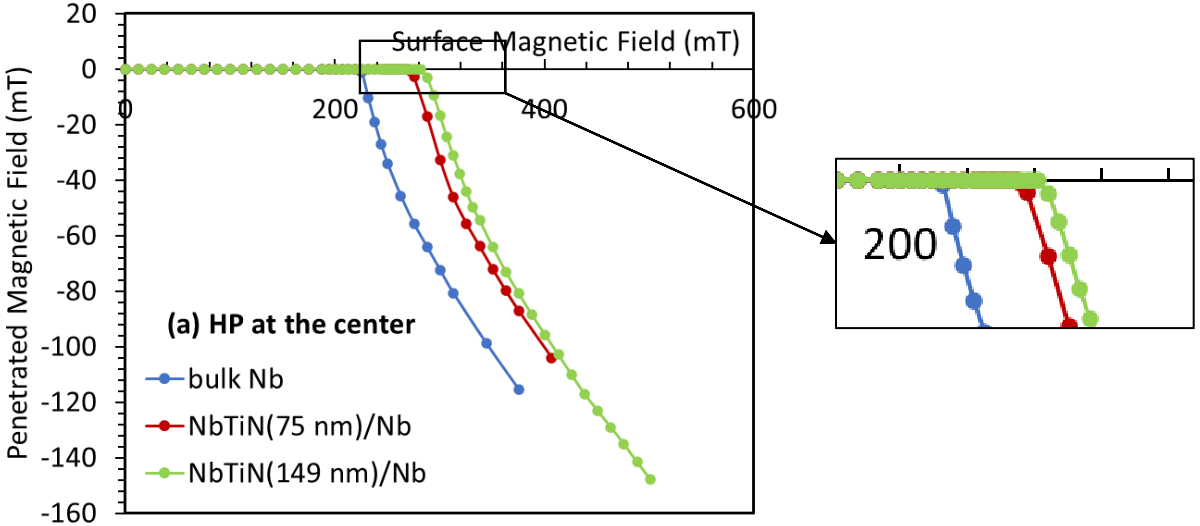


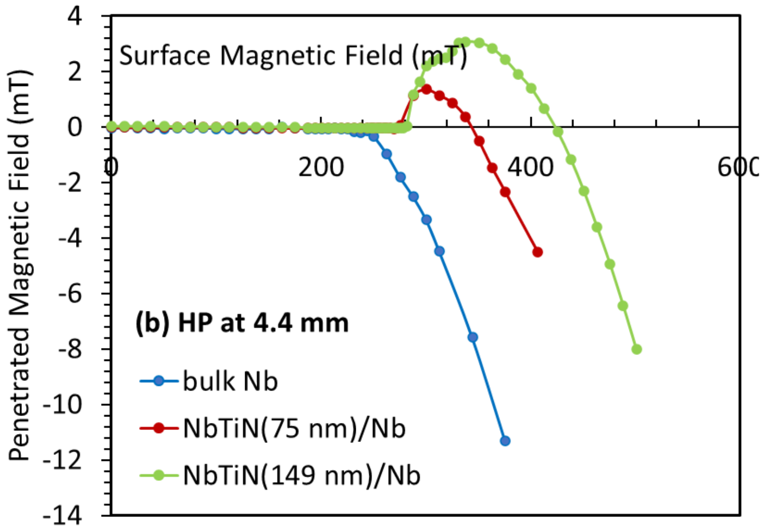


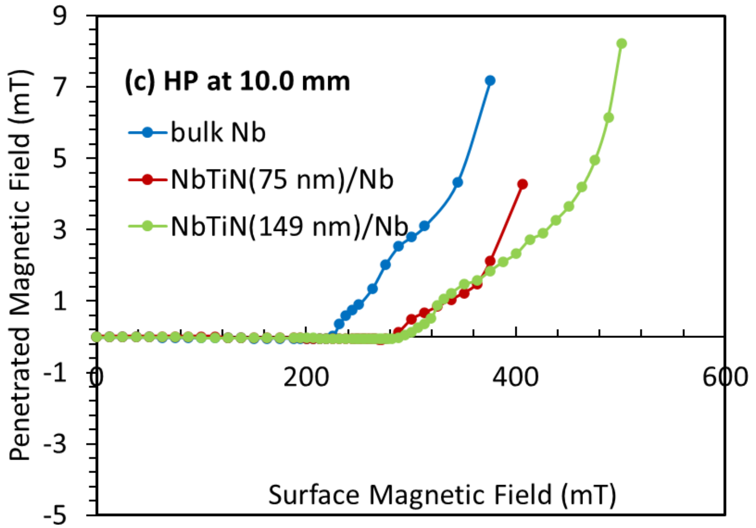

A Contour plot of **the maximum achievable peak surface field, $B_v$**

(a)

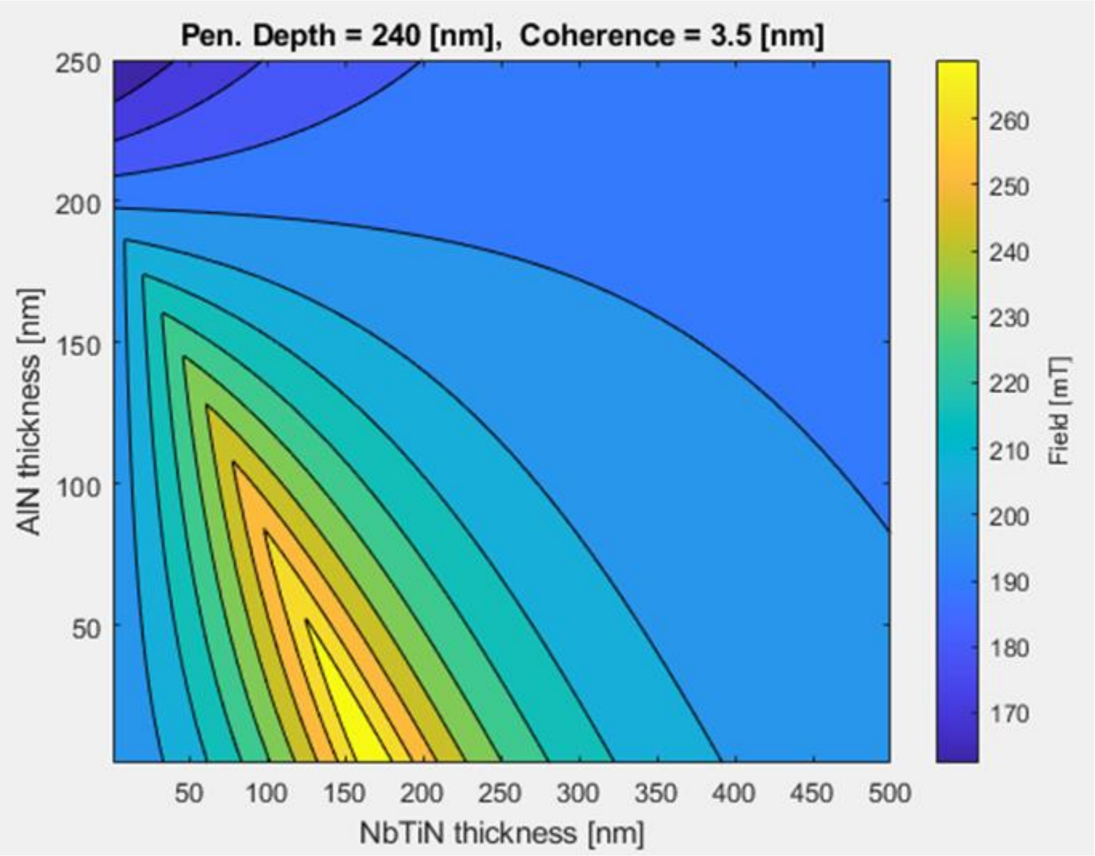


(b)

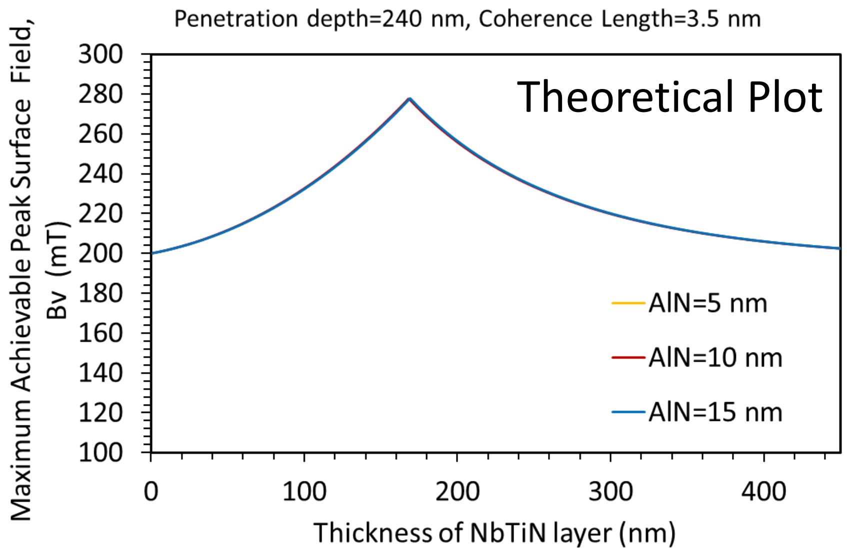


Equations in Ref. " T. Kubo, Y. Iwashita, and T. Saeki, Applied Physics Letters **104**, 032603 (2014)" are used for this contour plot

| Sample # | Thickness (nm) | |
|---|---|---|
| | NbTiN | AlN |
| 3 | 83 | ~10 |
| 4 | 166 | ~10 |
| 5 | 250 | ~10 |
| 6 | 371 | ~10 |

# NbTiN/AlN on Nb Substrate

## Magnetic Field Penetration Measurements
## At 4.35 K

| Sample # | Thickness (nm) | |
|---|---|---|
| | NbTiN | AlN |
| 3 | 83 | ~10 |
| 4 | 166 | ~10 |
| 5 | 250 | ~10 |
| 6 | 371 | ~10 |

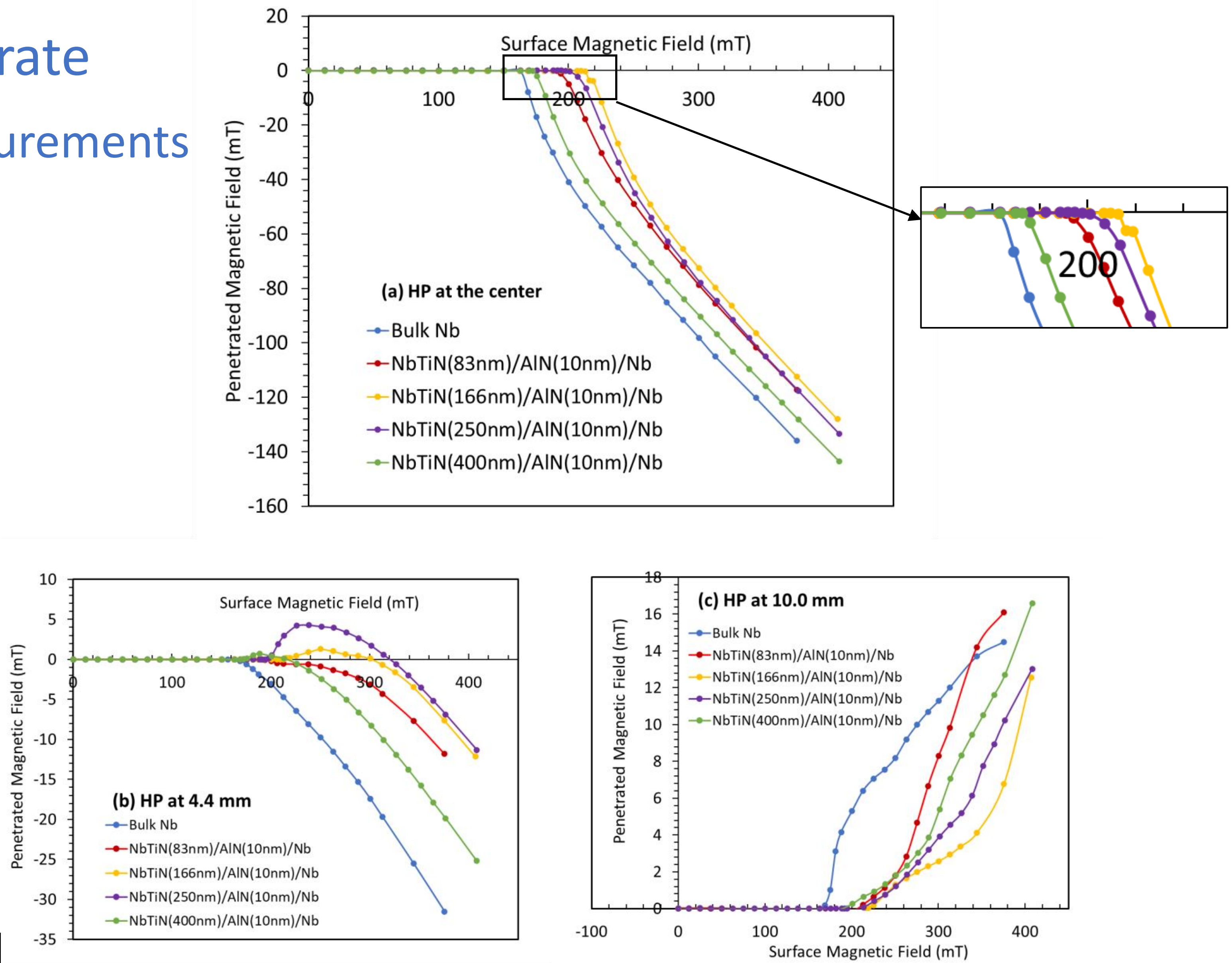

# NbTiN/AlN on Nb Substrate

## Magnetic Field Penetration Measurements At 2.00 K

| Sample # | Thickness (nm) | |
|---|---|---|
| | NbTiN | AlN |
| 3 | 83 | ~10 |
| 4 | 166 | ~10 |
| 5 | 250 | ~10 |
| 6 | 371 | ~10 |

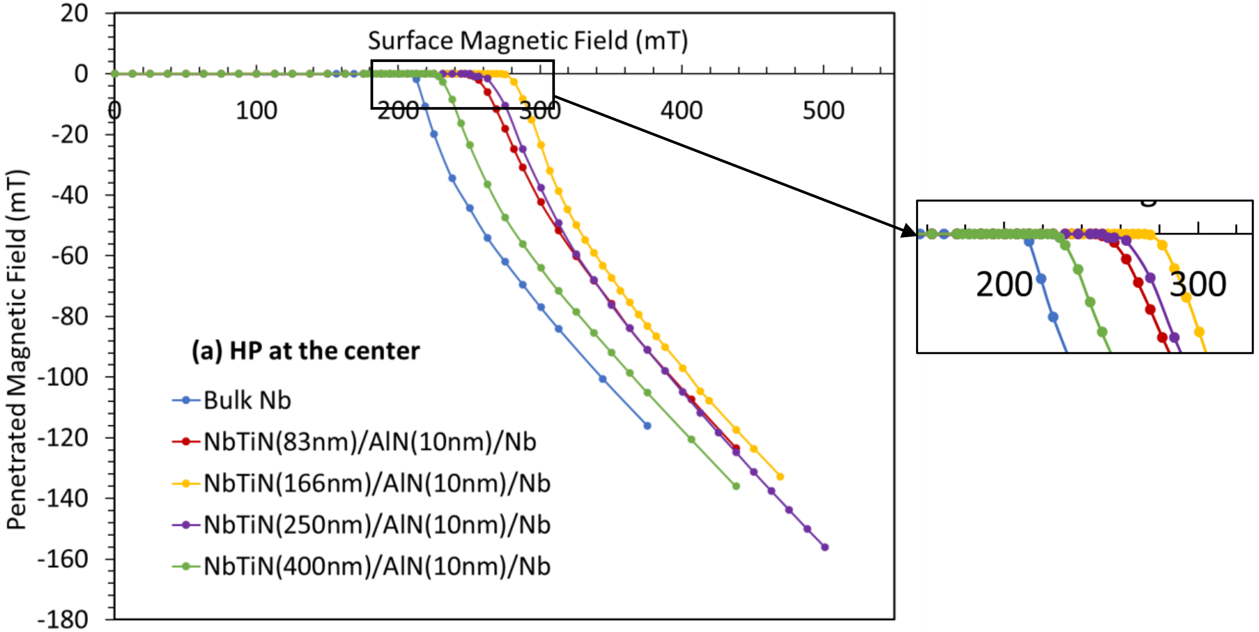


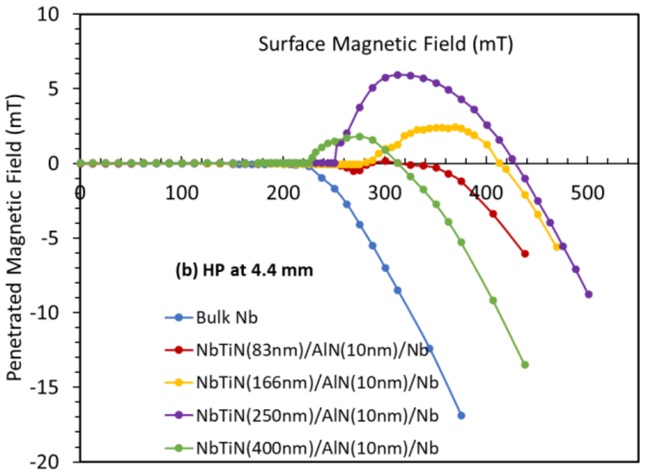


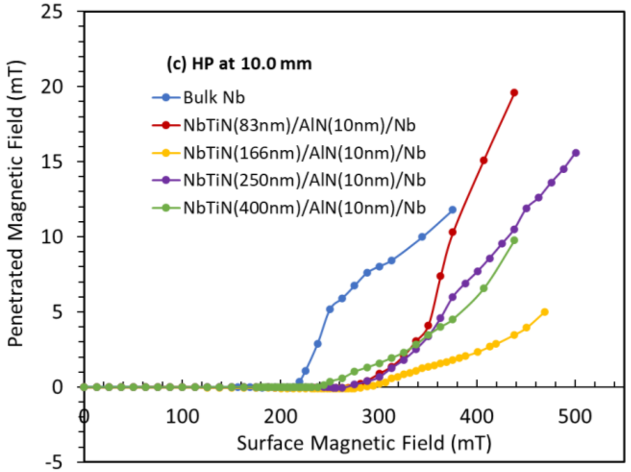

# The surface field at first full flux penetration, $B_p$ at 4.35 K and 2.00 K for different NbTiN layer thickness maintaining constant AlN layer thickness ~10 nm

| Sample # | Thickness (nm) | |
|---|---|---|
| | NbTiN | AlN |
| 3 | 83 | ~10 |
| 4 | 166 | ~10 |
| 5 | 250 | ~10 |
| 6 | 371 | ~10 |

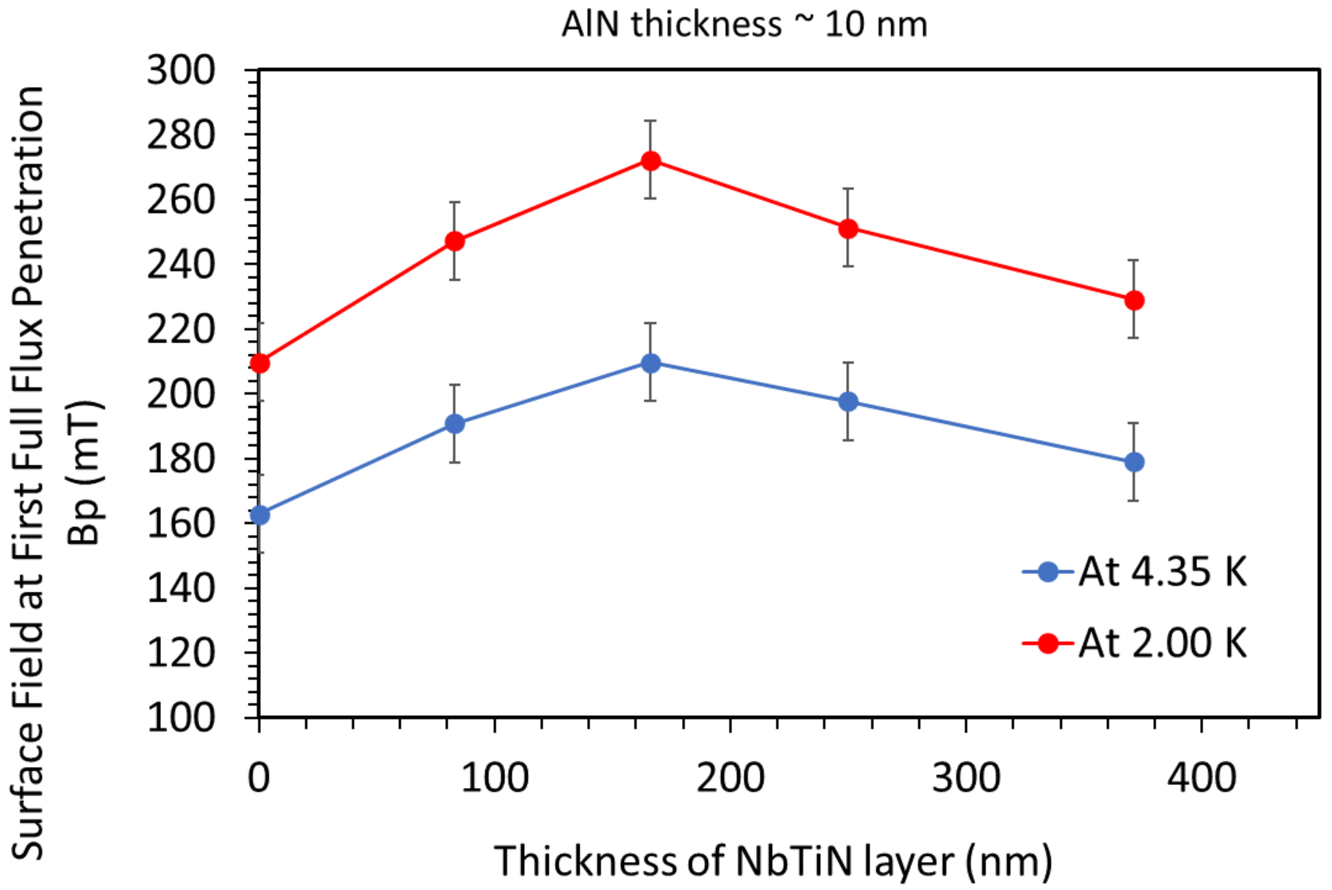


~25 % increase of Bp compared to bare Nb is observed with single NbTiN and single AlN layers on bulk Nb

A Contour plot of the maximum achievable peak surface field, $B_v$

(a)

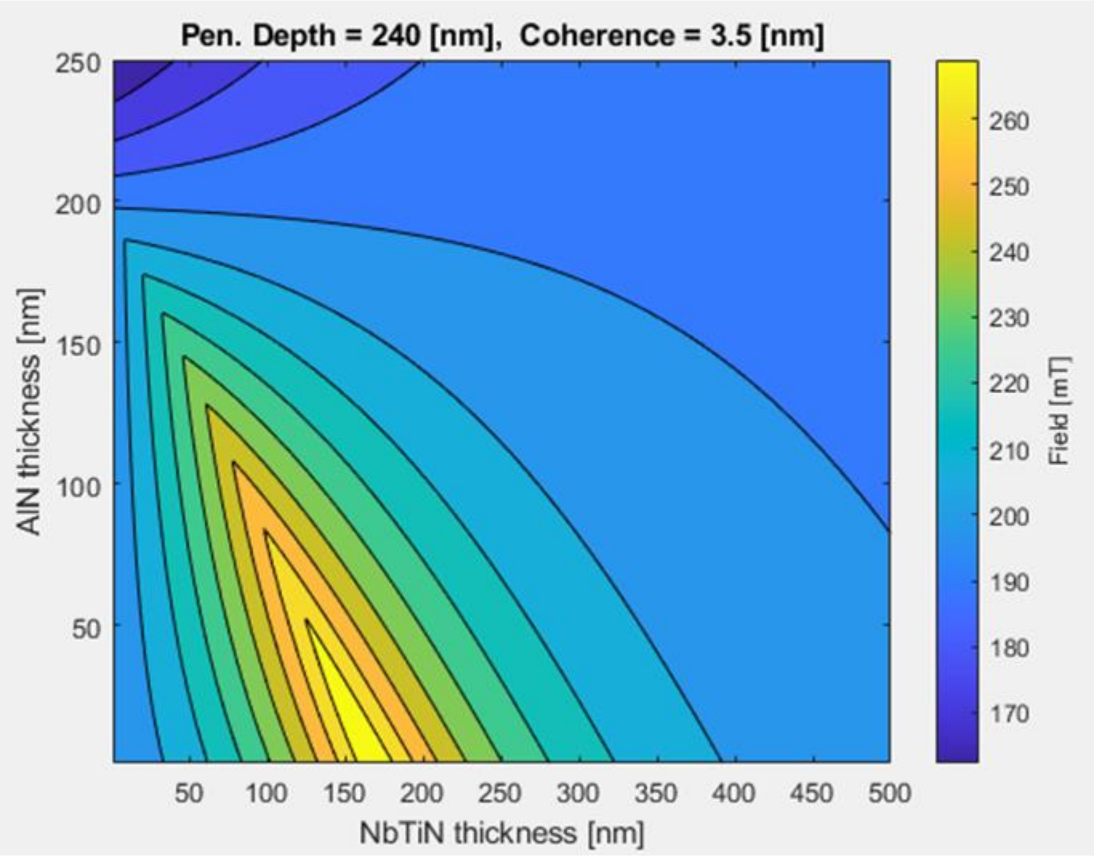


(b)

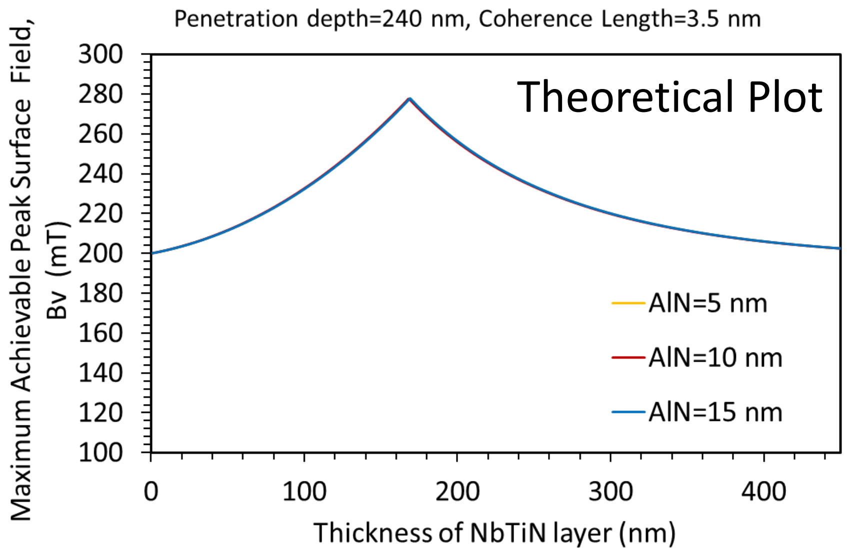


(c)

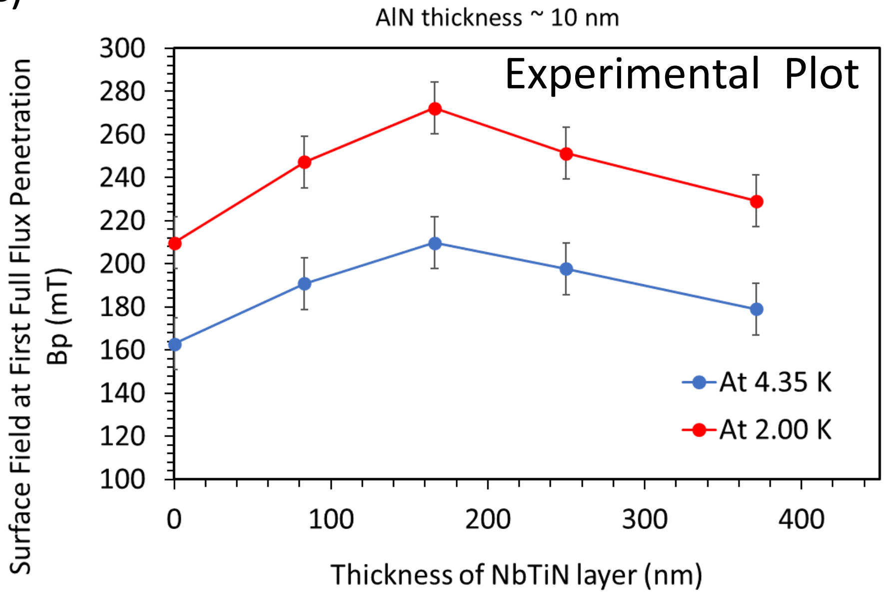


Equations in Ref. " T. Kubo, Y. Iwashita, and T. Saeki, Applied Physics Letters **104**, 032603 (2014)" are used for this contour plot

# The peak of the graph depends on the penetration depth and the coherence length of the sample.

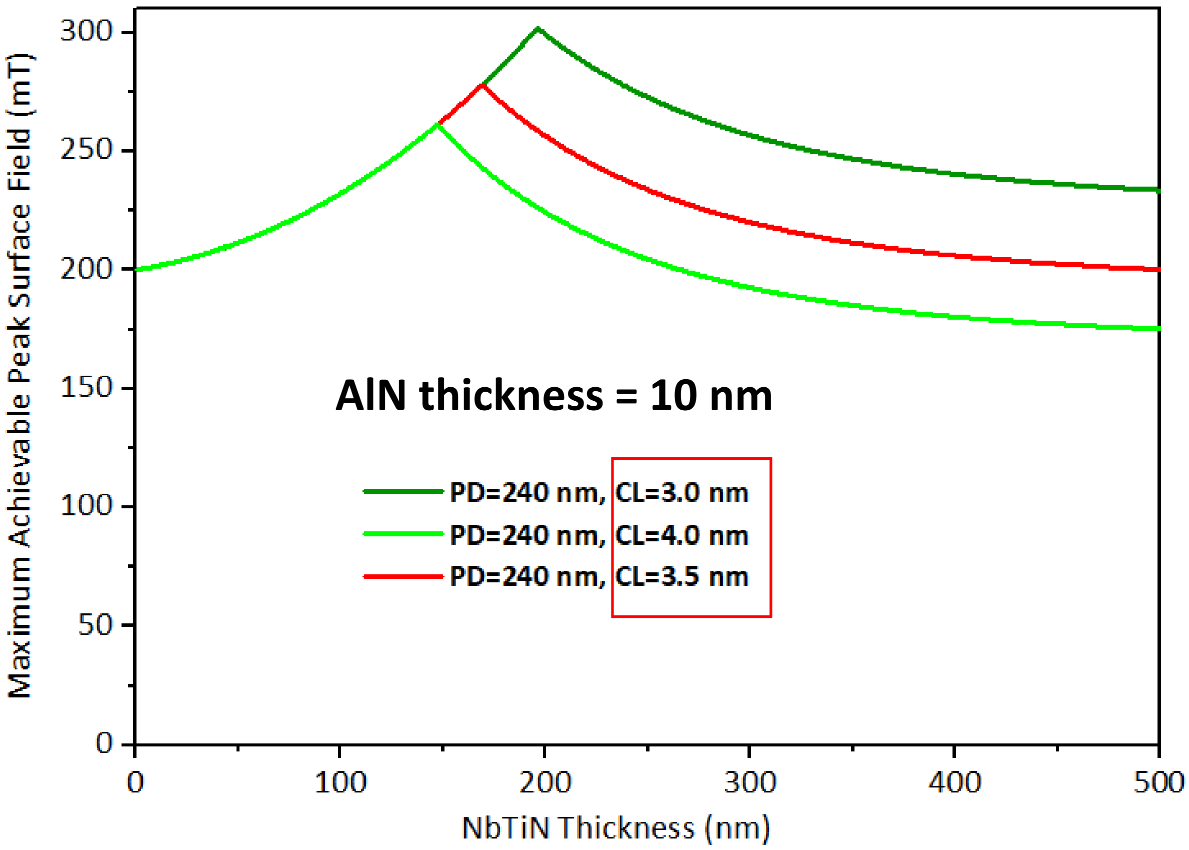


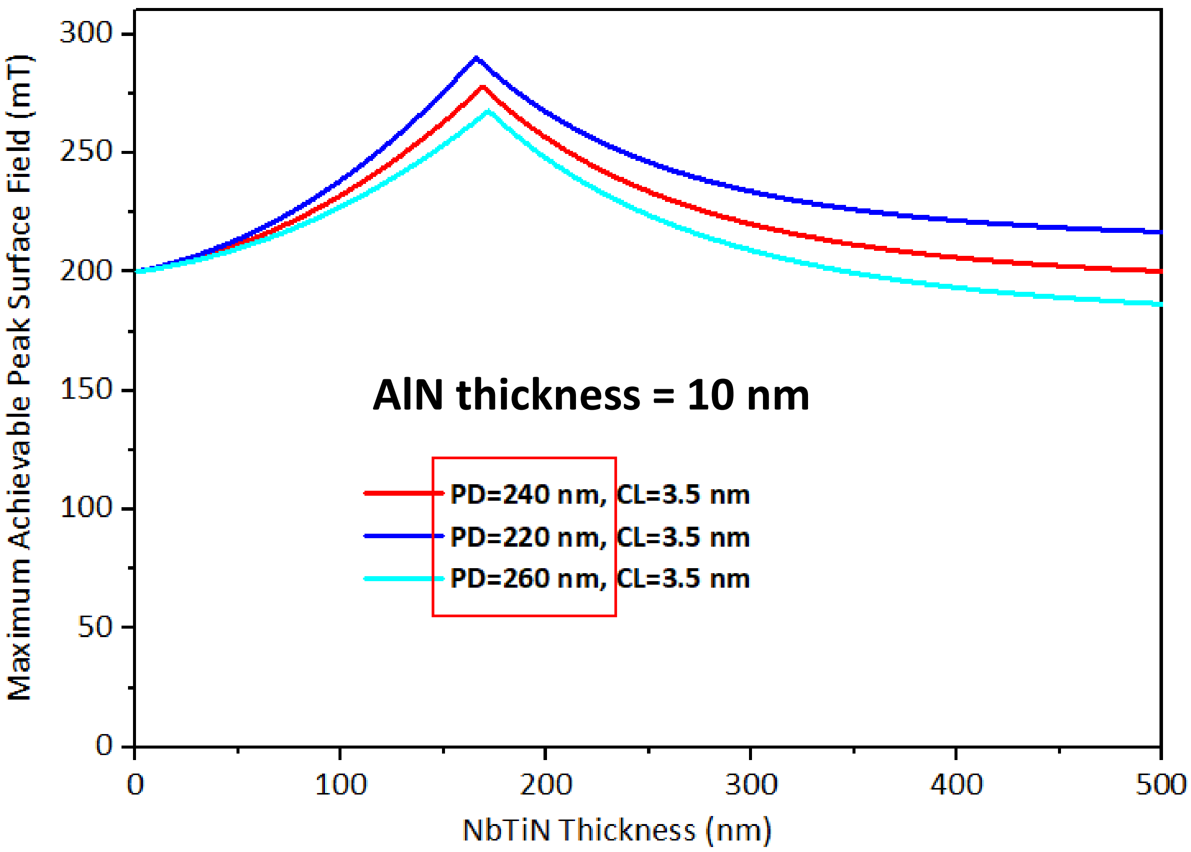

# Conclusions

- Layered Nb showed flux penetration at higher field compared to bare Nb.
- To explore multilayer concept that has been proposed to enhance peak surface magnetic field of the SRF cavity,

  a series of NbTiN/AlN coated on BCP Nb samples with
  - different NbTiN thickness
  - constant AlN thickness were tested.
- The variation of $B_p$ confirms that the existence of optimum thickness of S layer for maximum field and that is consistent with the theory build up in “T. Kubo, Y. Iwashita, and T. Saeki, Applied Physics Letters **104**, 032603 (2014)”.
- Optimum thickness of NbTiN for maximum *Bp* among measured four thicknesses is 166 nm when AlN is nearly 10 nm.

# Nb substrate with different roughness: BCP vs MP+ EP

Optical Images

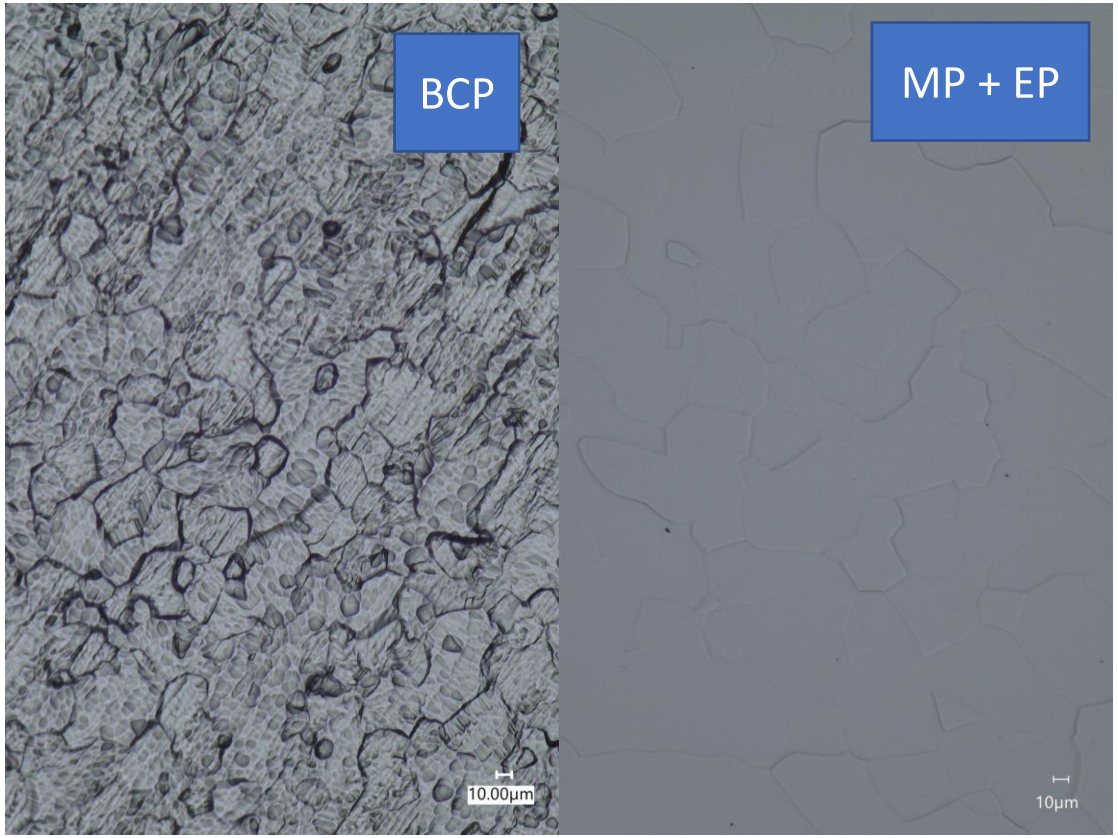


RMS roughness: ~ 3 µm ~ 20 nm
Substrate thickness ~ 250 um 150 um

BCP- Buffered Chemical Polishing
EP - Electropolishing
MP- Mechanical Polishing

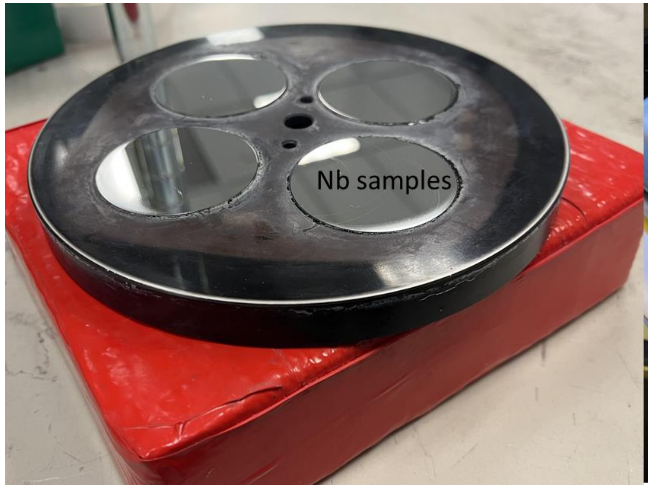


Mirror finished samples

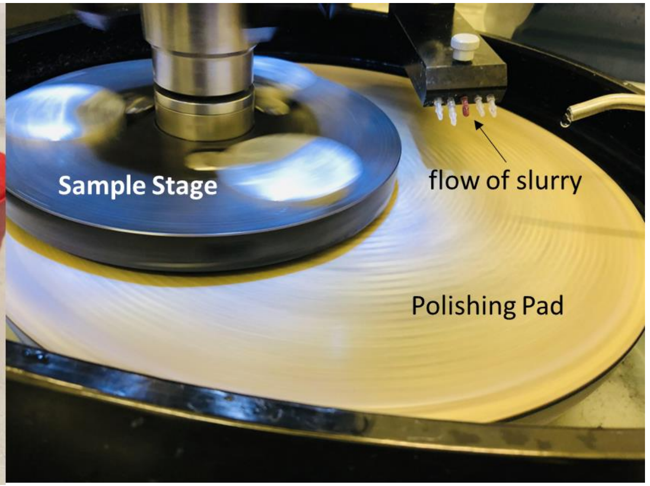


Sample stage is spinning on polishing pad with flow of slurry

# NbTiN/AlN coated on MP+EP Nb substrate

| Sample # | Thickness (nm) | |
|---|---|---|
| | NbTiN | AlN |
| 5 | 250 | ~10 |
| 6 | 371 | ~10 |

5-10 % increase is estimated compared to multilayer coated on BCP Nb

Magnetic Field penetration measurements

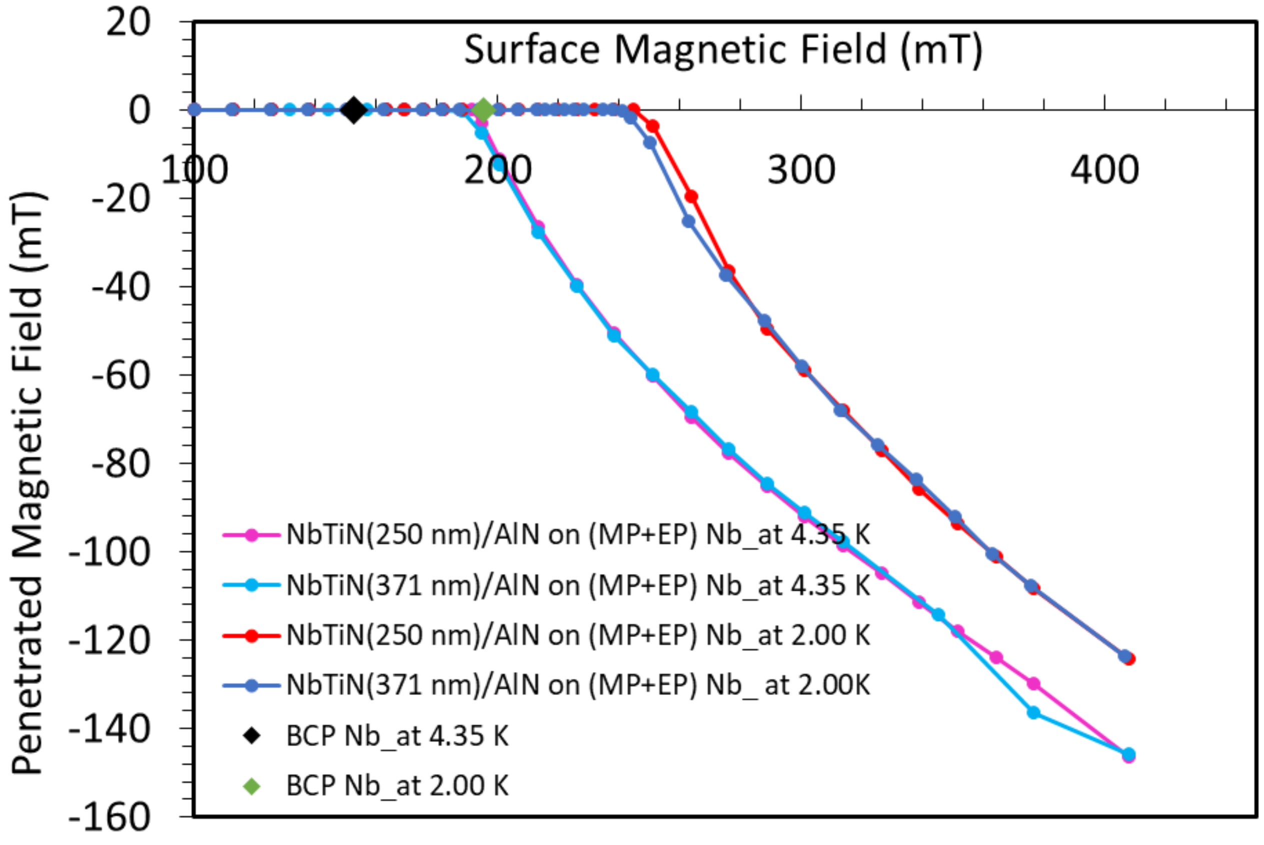

- Prof. Jean Delayen
- Prof. Alex Gurevich
- Prof. Anne-Marie Valente Feliciano
- Prof. Moskov Amaryan and Prof. Khan Iftekharuddin
- Dr. Gigi Ciovati
- Read Beverstock, Eric Lechner, Carrie Baxley
- Junki Makita and Salvador Sosa
- Nizam Sayeed and Chris Sundahl
- Department of Physics, ODU
- SRF and machine shop staff at Jefferson Lab
- My family and friends
- NSF (Grants PHY-1734075 and PHY-1416051) and DOE (Awards DE-SC0010081 and DE-SC0019399)


# Thank You !